2005 International Linear Collider Physics and Detector Workshop

and Second ILC Accelerator Workshop

Snowmass, 14 - 27 August 2005

Physics potential of vertex detector as function of beam pipe radius

Sonja Hillert, Chris Damerell

(on behalf of the LCFI collaboration)

Introduction

aim: optimise design of vertex detector and evaluate its physics performance

b quark sign selection is a powerful physics tool, enabling the measurement of asymmetries which would otherwise be inaccessible, and for background reduction in multi-jet processes

b quark sign can be obtained in a very clean way from that of the B hadron, if the B hadron is charged; in those cases, one needs to measure the vertex charge, given by the total charge of the particles in the B decay chain

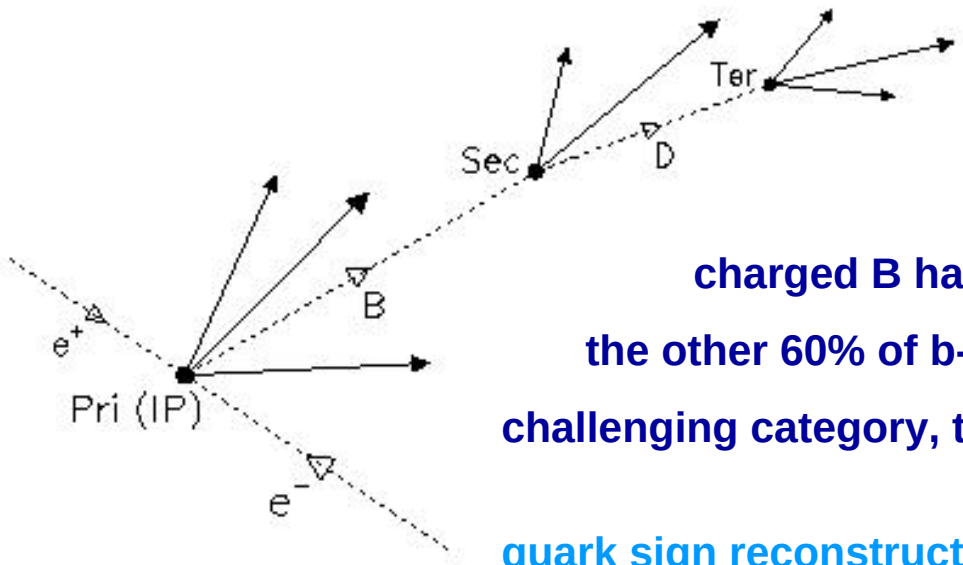

~ 40% of b-quarks hadronise to yield charged B hadrons, allowing this measurement – the other 60% of b-quarks, yielding neutral B's, form a more challenging category, to be studied later (e.g. using SLD charge dipole)

quark sign reconstruction could give access to new physics, if done carefully – encouraging results have already been demonstrated by SLD

Introduction

Study jets from $e^+e^- \to \gamma Z \to b\bar{b}$ events, using fast simulation SGV for detector description;

performance of vertex charge reconstruction, measured by the probability of reconstructing a neutral b-hadron as charged, studied as function of energy and polar angle

focus on comparison of detectors with three different beam pipe radii: 8, 15 and 25 mm

also compare vertex detectors of the SiD, GLD and the LDC detector concepts

(both inserted into the LDC 'global detector', to decouple vertex detector from other effects)

Vertex charge as a tool for physics

S. Riemann,

LC-TH-2001-007

Example 1: left-right forward-backward asymmetries in $b\bar{b}$ events

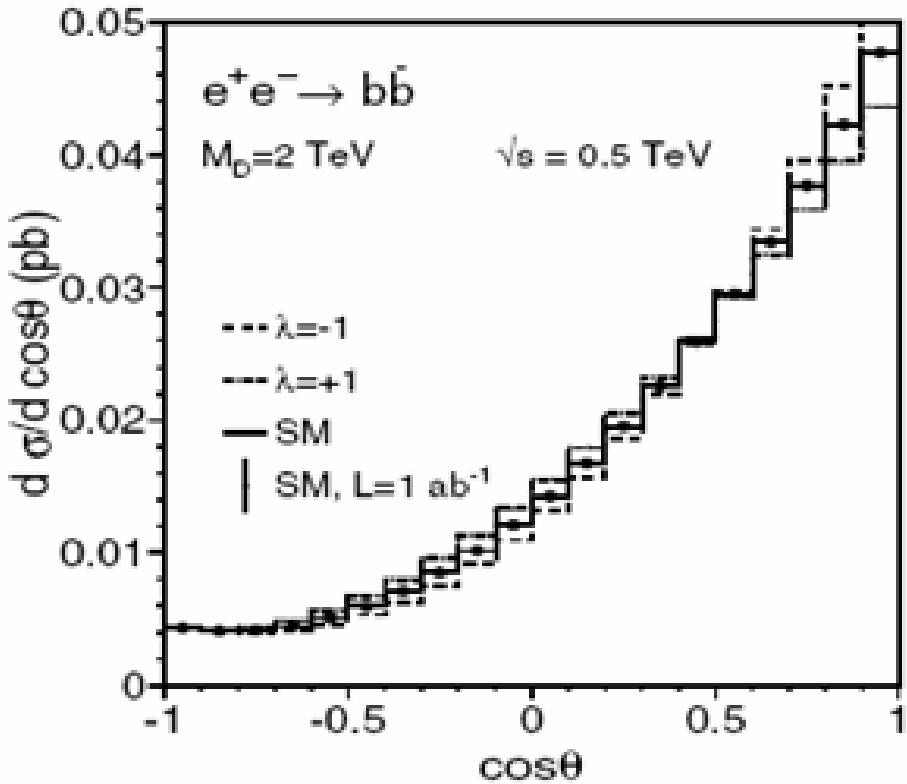

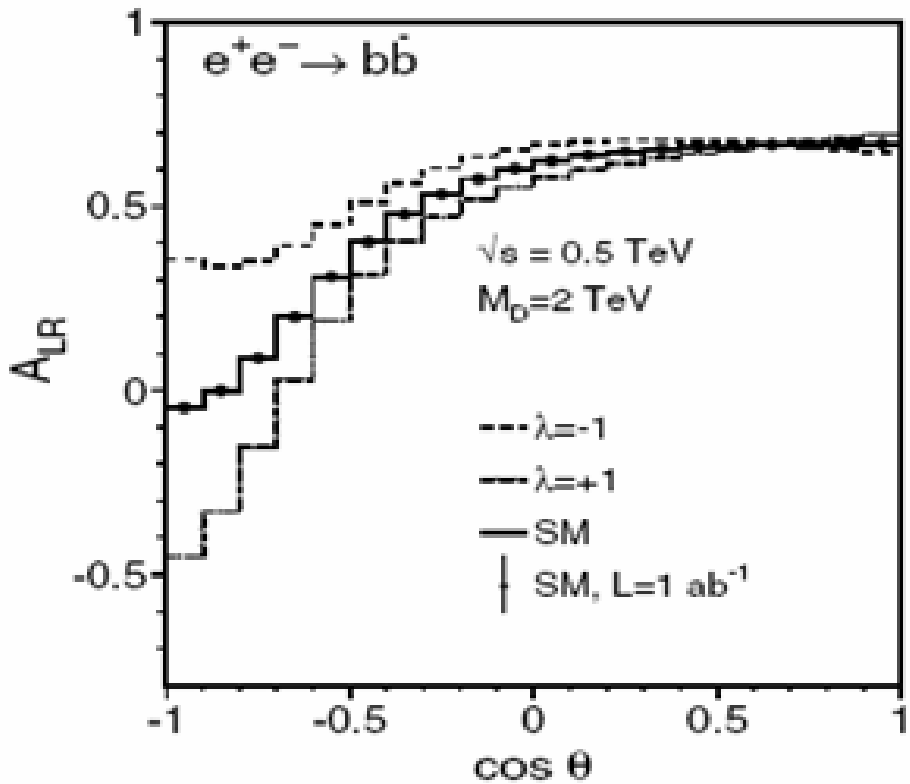

- model dependence predicted in cos θ region where cross section is small

  → challenging measurement

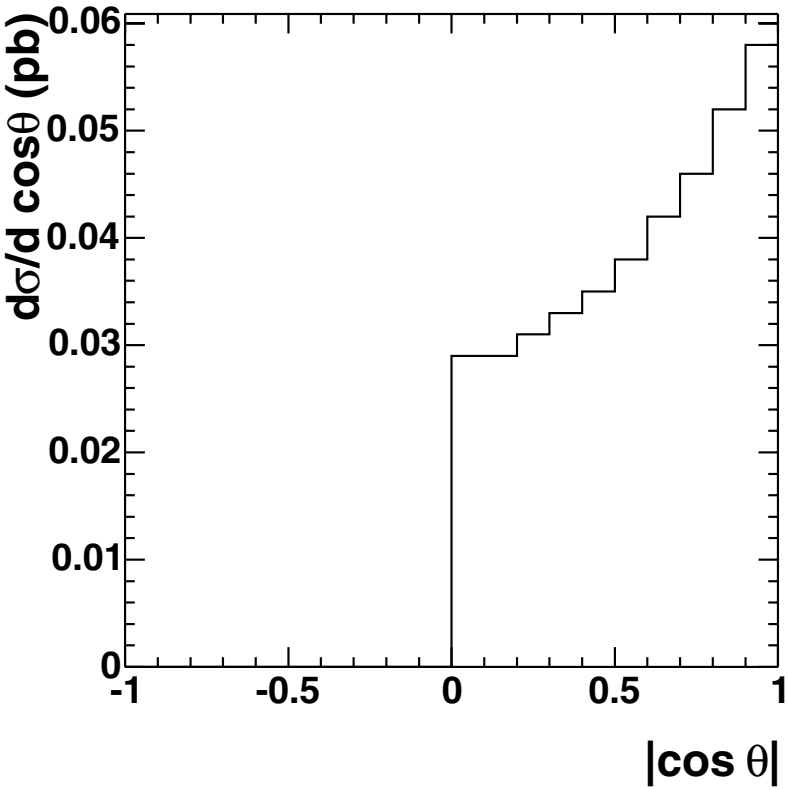

without quark sign selection

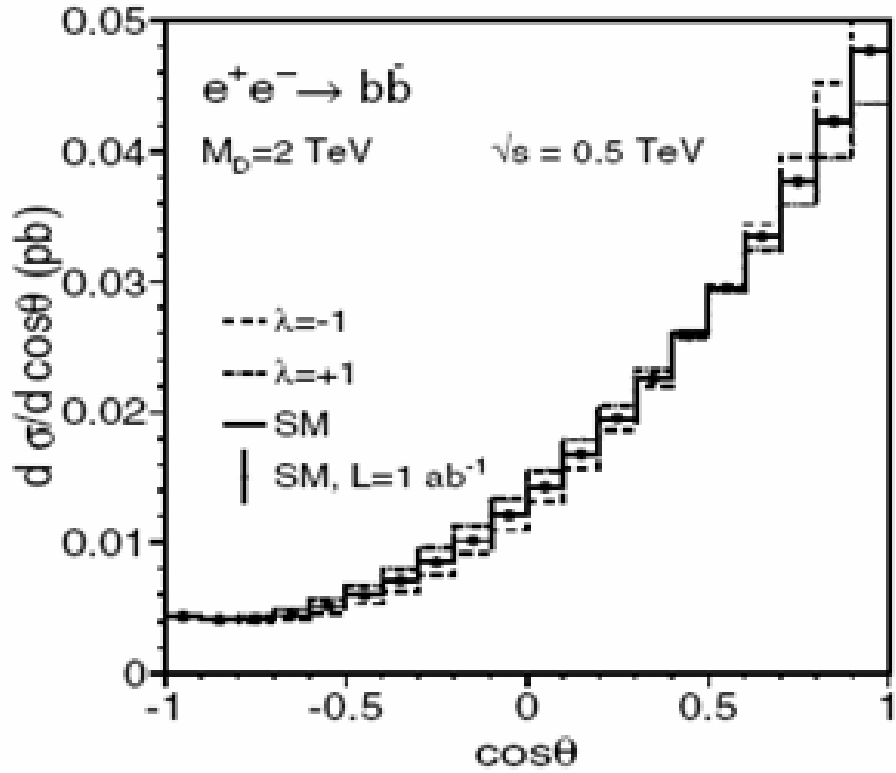

with perfect quark sign selection

- **vertex charge allows unfolding angular distributions by tagging events with b or bbar in the forward region,**
- **neutral B's from dominant forward region wrongly reconstructed as charged are the main source of background**

Vertex charge as a tool for physics

Example 2: there are numerous multi-jet processes requiring sign selection of

$e^+e^- \to t\bar{t}$
$\quad \hookrightarrow bW$
$\quad\quad \hookrightarrow c\bar{s}$

use of s-bar jet direction to analyse t polarisation

$e^+e^- \to \tilde{\chi}_2^0 \tilde{\chi}_1^0$
$\quad \hookrightarrow \tilde{\chi}_1^0, \; q\bar{q}$

spin correlations

$e^+e^- \to ZHH$

angular analysis

Performance for jets over a wide range of energies and the full angular range is relevant.

Vertex charge reconstruction

Vertex charge reconstruction studied using jets from $e^+e^- \to \gamma Z \to b\bar{b}$ varying sqrt(s),

select two-jet events with jets back-to-back

- **need to find all stable B decay chain tracks – procedure:**
- **run vertex finder ZVTOP: the vertex furthest away from the IP ('seed') allows to define a vertex axis**
  → reduce number of degrees of freedom
- **cut on L/D, optimised for each detector configuration, used to assign tracks to the B decay chain**

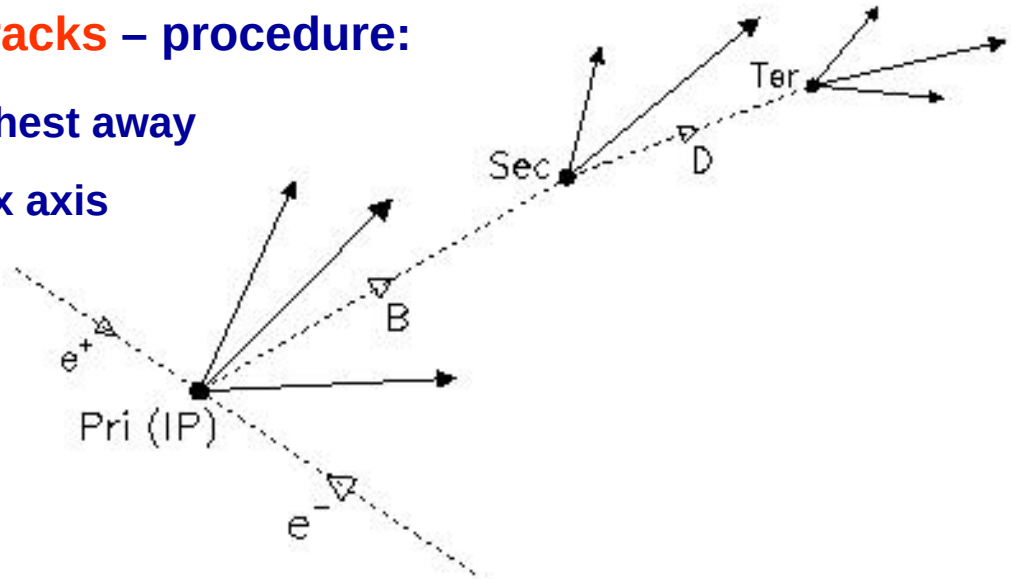

- **by summing over these tracks obtain Q_{sum} (charge)**

- **vertex charge** $Q_{Vtx,r} = \begin{cases} +1 \text{ for } Q_{sum} = +1 \text{ or } +2 \\ -1 \text{ for } Q_{sum} = -1 \text{ or } -2 \end{cases}$

Leakage rates

- define leakage rates as probabilities
  - λ_{pm}: prob. of charged vertex being reconstructed as neutral and
  - λ_0: prob. of neutral vertex being reconstructed as charged

- λ_0 measures the 'leakage rate' of bbar jets which appear as b-jets and vice versa

  → λ_0 is hence the quality parameter for the vertex charge analysis

Varying the centre of mass energy

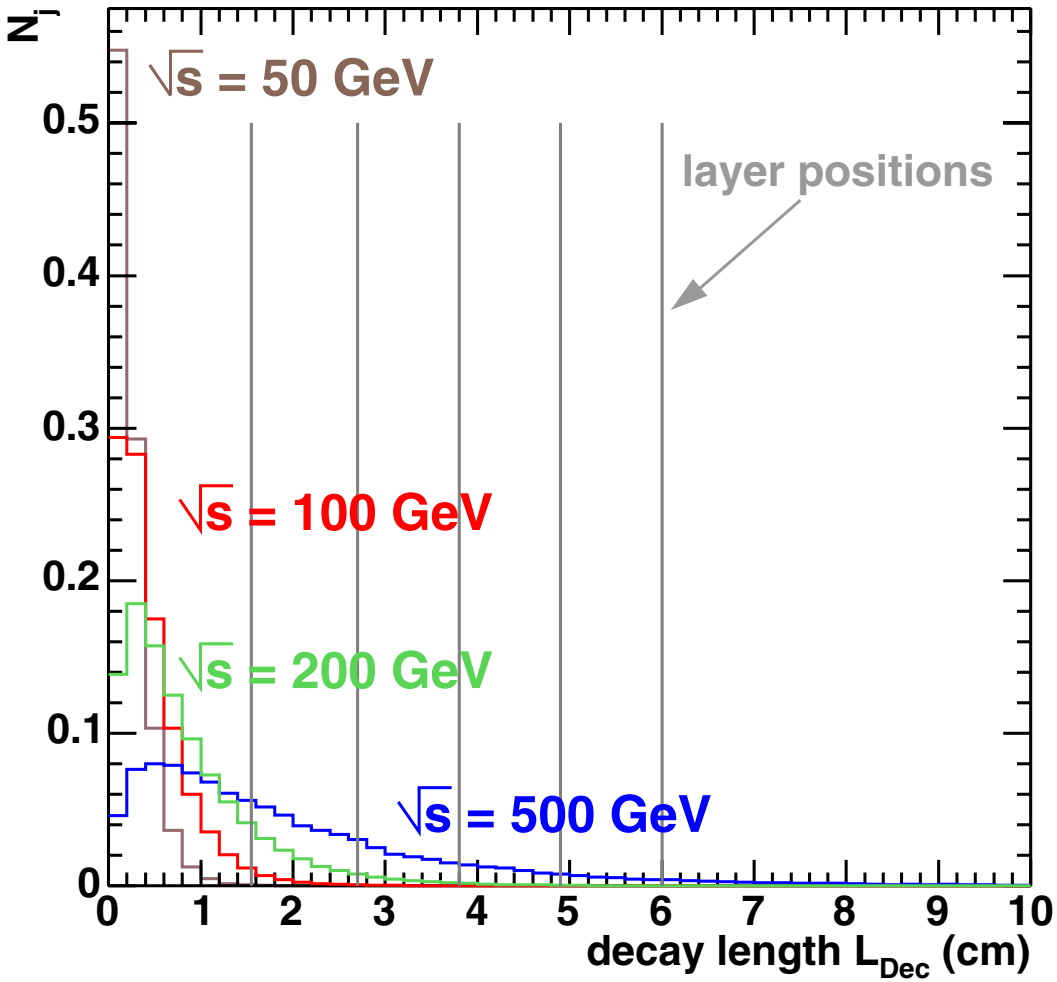

At low energy:

- **lower average track momentum**
  - → **more strongly affected by multiple scattering**
- **seed vertex on average closer to IP**
  - → **track assignment more challenging, although on average more hits / track available**

→ **expect performance to become worse at lower energy**

Position of vertices wrt detector layers: percentages

CM energy (GeV)	50	100	200	500
inside beam pipe	99.99 %	99.49 %	94.69 %	74.49 %
between layer 1 & layer 2	0.01 %	0.48 %	4.48 %	14.95 %
between layer 2 & layer 3	--	0.02 %	0.67 %	5.78 %
between layer 3 & layer 4	--	--	0.11 %	2.49 %
between layer 4 & layer 5	--	--	0.04 %	1.11 %
outside vertex detector	--	--	0.01 %	1.19 %

MC-level secondary vertex

CM energy (GeV)	50	100	200	500
inside beam pipe	95.39 %	93.97 %	85.89 %	57.64 %
between layer 1 & layer 2	0.53 %	1.37 %	7.82 %	20.83 %
between layer 2 & layer 3	0.42 %	0.34 %	1.46 %	9.03 %
between layer 3 & layer 4	0.33 %	0.27 %	0.43 %	4.32 %
between layer 4 & layer 5	0.32 %	0.23 %	0.21 %	2.10 %
outside vertex detector	3.00 %	3.82 %	4.18 %	6.08 %

MC-level tertiary vertex

Seed decay length dependence of leakage rate

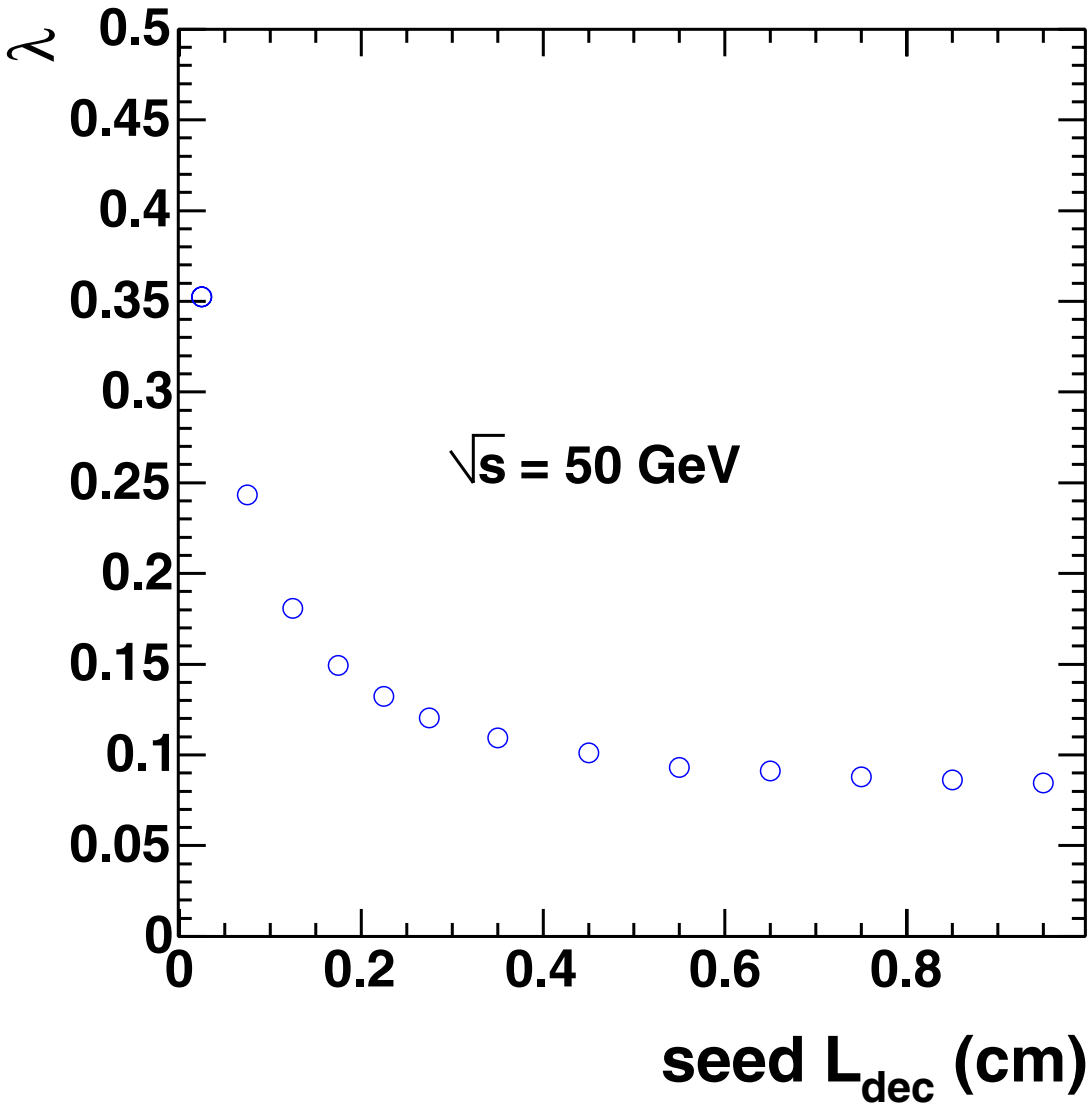

- at low seed vertex decay length, rise in probability of confusing B decay chain with IP tracks
  → strong increase in leakage rate

Polar angle dependence at different CM energies

- at lower energies, average track momentum is lower
  - → more strongly affected by multiple scattering
  - → central part of the detector shows worse performance and 'detector edge' effects set in at lower cos θ

→ at higher energies, performance stays excellent out to large values of cos θ

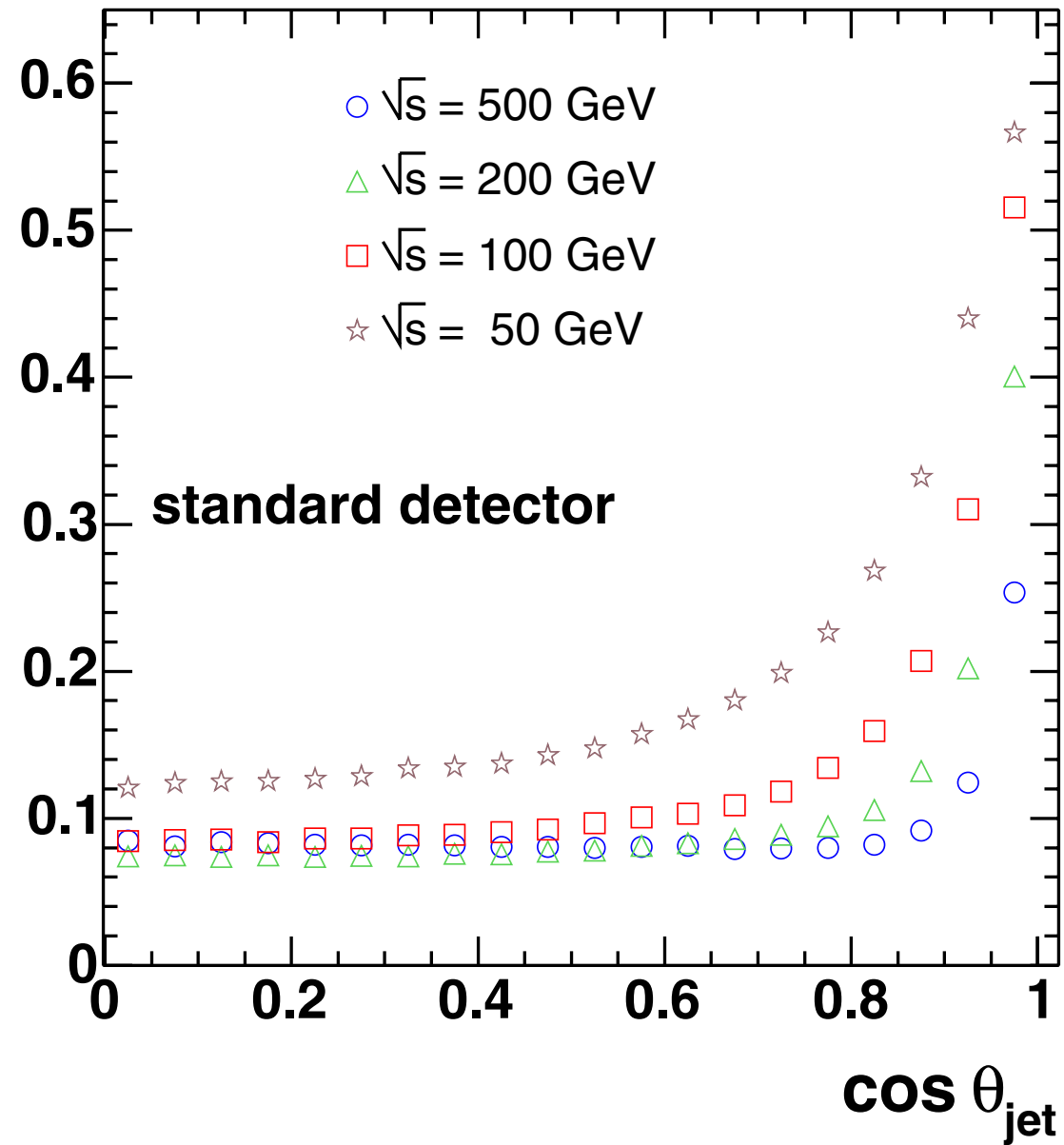

Varying the beam pipe radius

Compare 3 detectors with different inner layer radius:

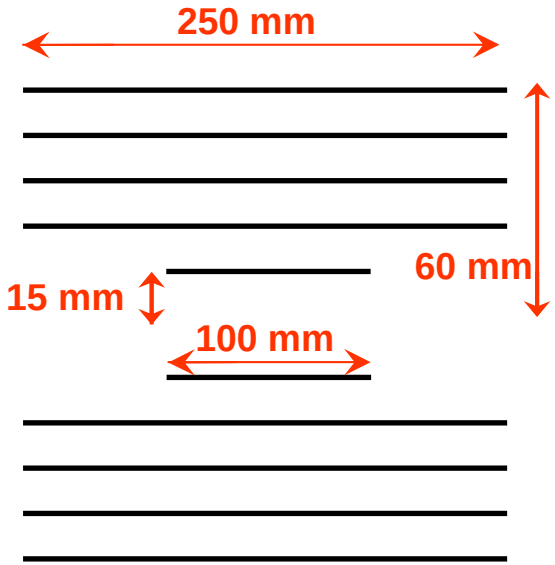

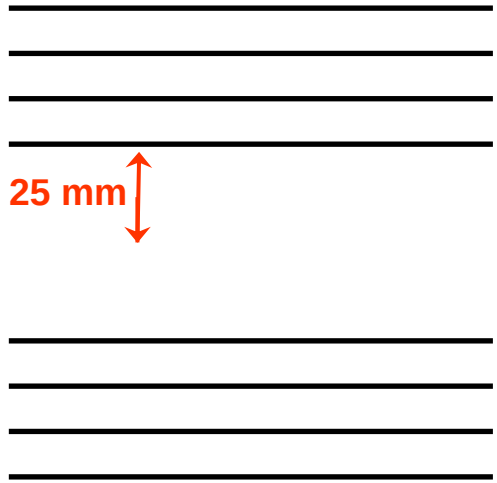

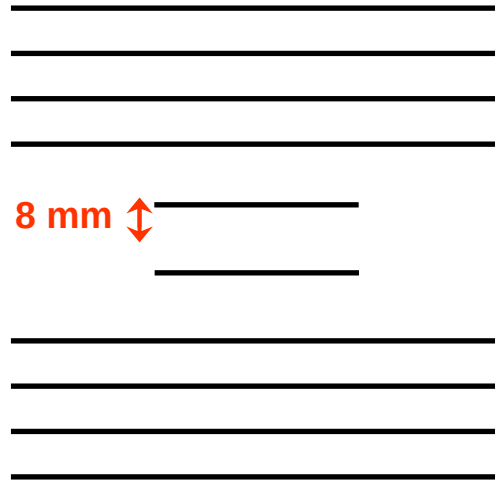

standard detector:

R_{bp} = 15 mm, thickness 0.4 mm

innermost layer at 15.5 mm;

layer thickness 0.1 % X_0

(same for all detectors)

large R_{bp} detector:

R_{bp} = 25 mm, thickness 1 mm

innermost layer removed

new inner layer at 25.5mm

has full length of 250 mm

small R_{bp} detector:

R_{bp} = 8 mm, thickness 0.4 mm

innermost layer moved inwards

to 8.5 mm, positions of other

layers retained

Note that the beam pipe probably has to be made thicker if its radius is increased

Optimising the L/D cut

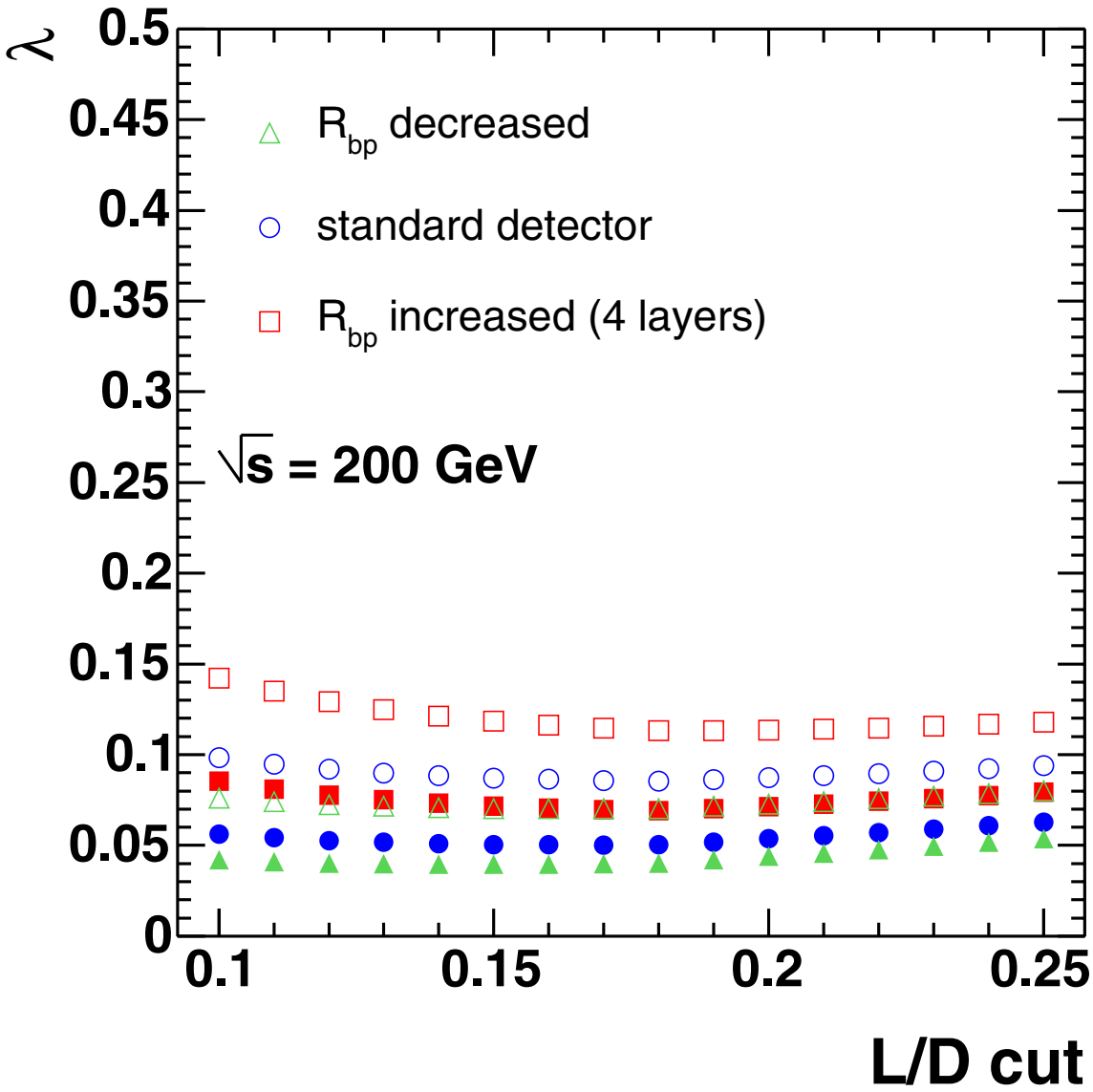

- leakage rates vary little with $(L/D)_{min}$ near the minimum value, energy dependence small
- for each detector $(L/D)_{min}$ is optimised at sqrt(s) = 200 GeV integrating over the range $30^{o} < \theta < 150^{o}$
- resulting cut values are
  - small R_{bp} detector: $(L/D)_{min} = 0.17$
  - standard detector: $(L/D)_{min} = 0.18$
  - large R_{bp} detector: $(L/D)_{min} = 0.19$

Polar angle dependence for different R_{bp} values

- consider CM energy of 100 GeV, corresponding to jet energy of 50 GeV (common in multi-jet events):

- difference of detectors in performance stable over plateau region,
  ~ 0.03 between standard, large R_{bp} det.
  ~ 0.02 between standard, small R_{bp} det,
  where λ_0 ~ 0.095 for standard detector

- towards the edge of the detector, difference between detectors increases, to ~ 0.10 between large & small R_{bp} det., with relative difference between standard detector and large R_{bp} det decreasing

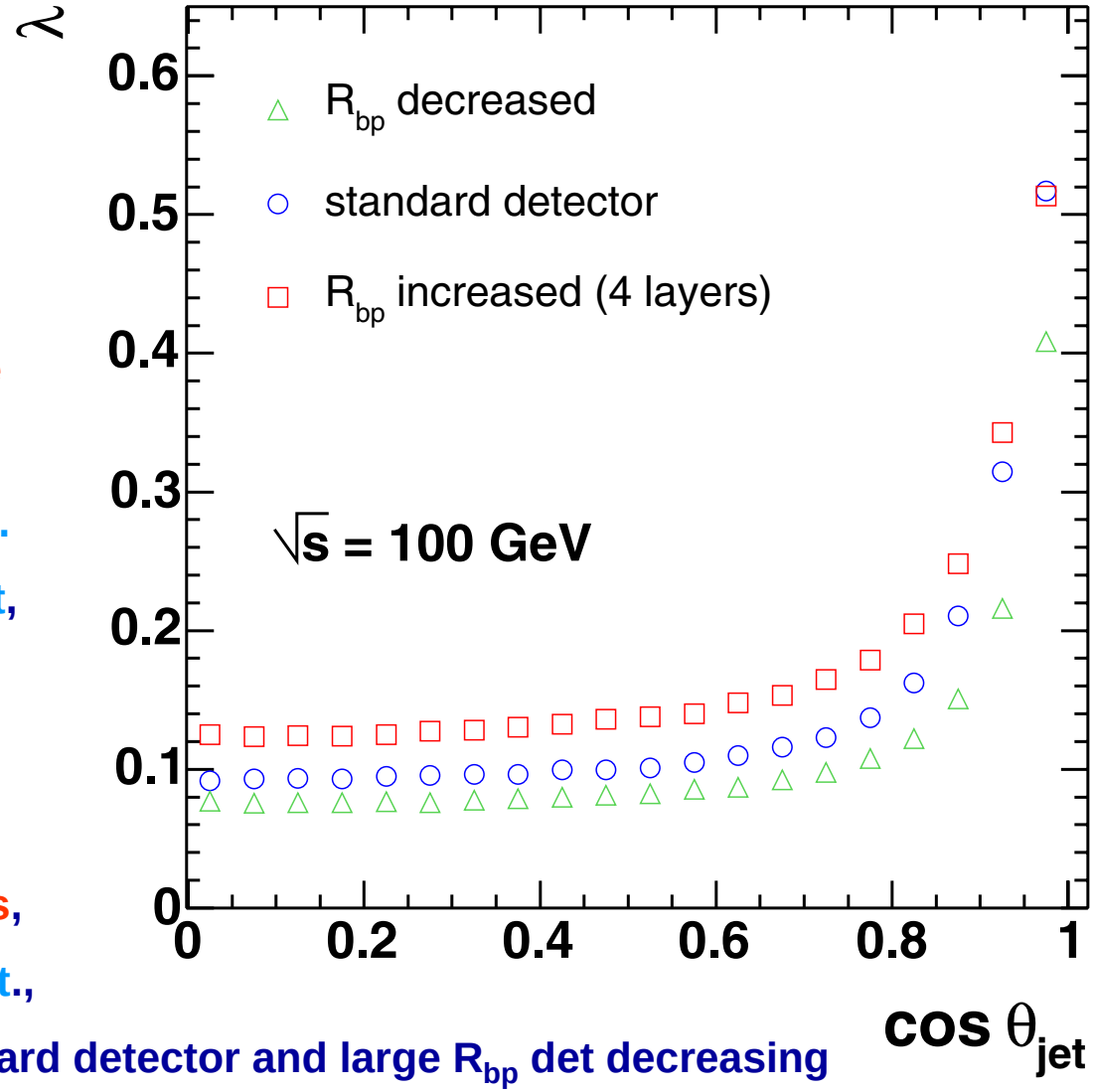

Energy dependence for different R_{bp} values

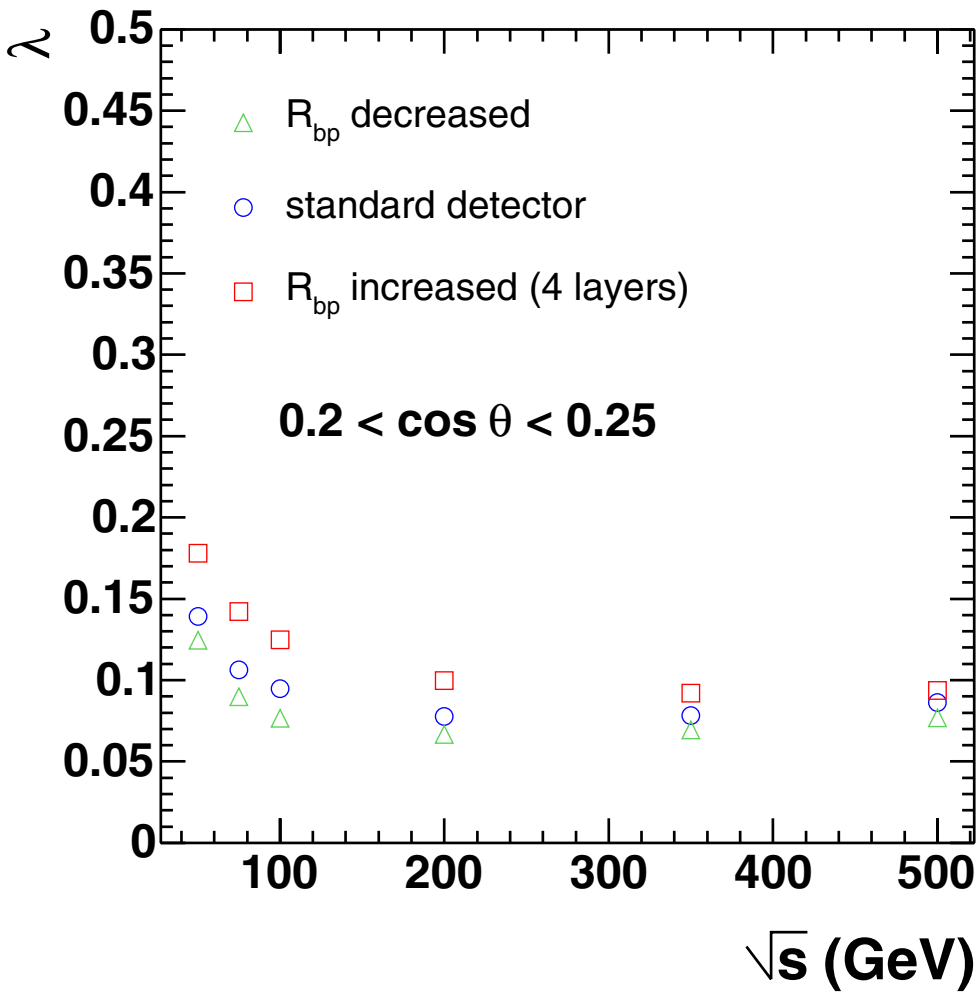

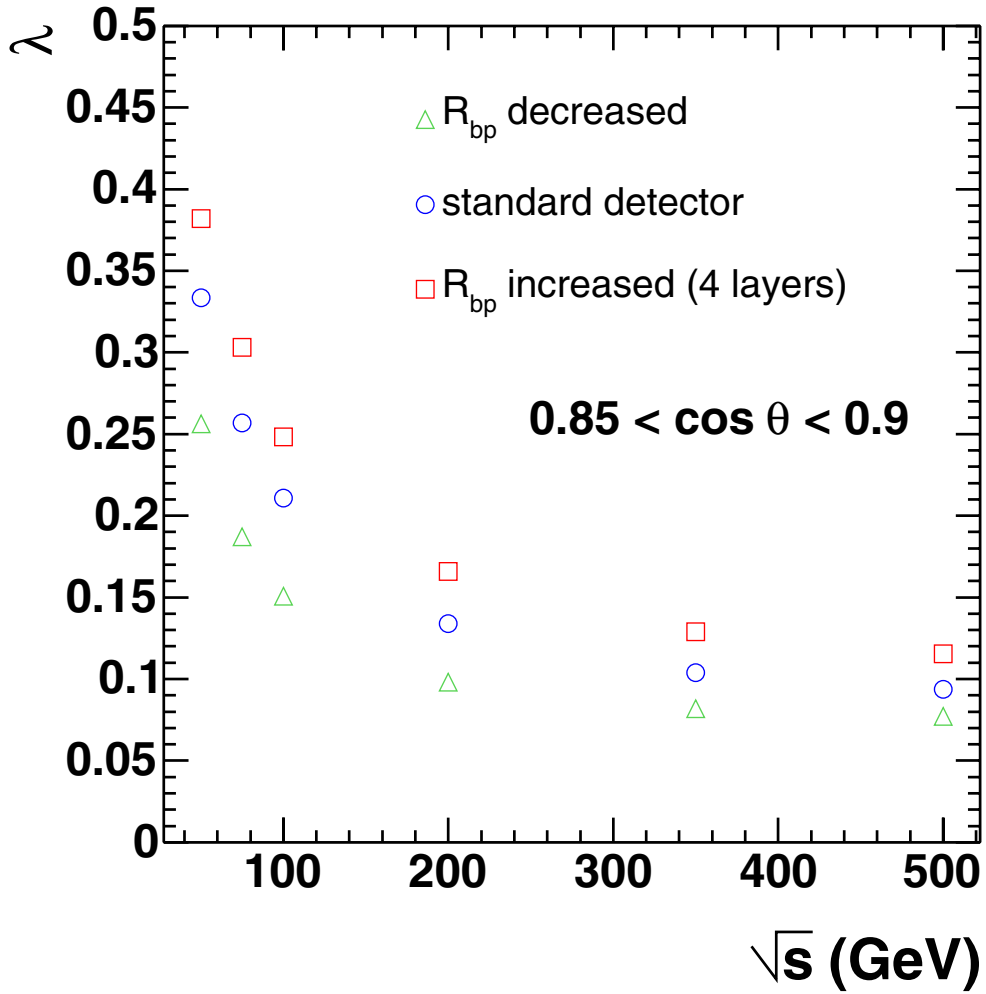

in central part of the detector, difference between standard and large R_{bp} detector is more pronounced, at the detector edge, difference between standard & small R_{bp} detector is larger

Average leakage as function of CM energy

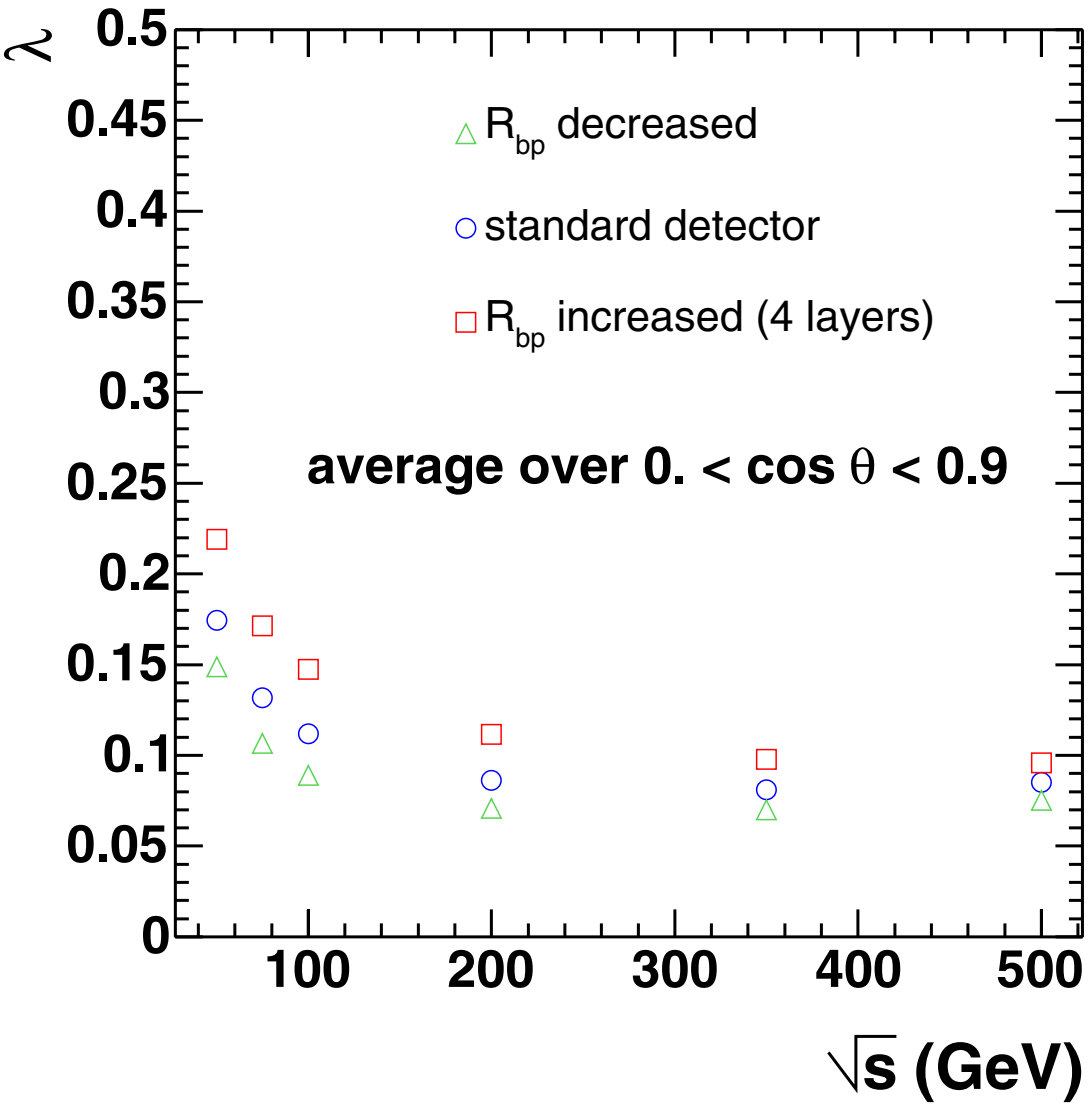

- **in multijet events, performance has to be good over full angular range → average over cos θ region (0, 0.9)**
- **both λ_0 and difference in λ_0 between detectors increase towards lower energies**

Attempt at estimating effective luminosities from λ_0

- define luminosity factor as the factor by which the integrated luminosity needs to be changed in order to measure the signal with the same statistical significance with modified detector compared to the standard detector

  i.e. measured signal / σ(signal) is equal

- N-jet luminosity factor $f_{L,N}$ is applicable to analyses, in which vertex charge needs to be reconstructed for N jets

Attempt at estimating effective luminosities from λ_0

first estimate of luminosity factors obtained as follows:

leakage rate large at low seed decay lengths

by increasing cut on decay length to $L_{dec,equiv}$, can improve performance of the large R_{bp} detector, until λ_0 agrees with that of the standard detector

increasing the cut results in loss in efficiency

→ need larger integrated luminosity to obtain sample of same statistical significance

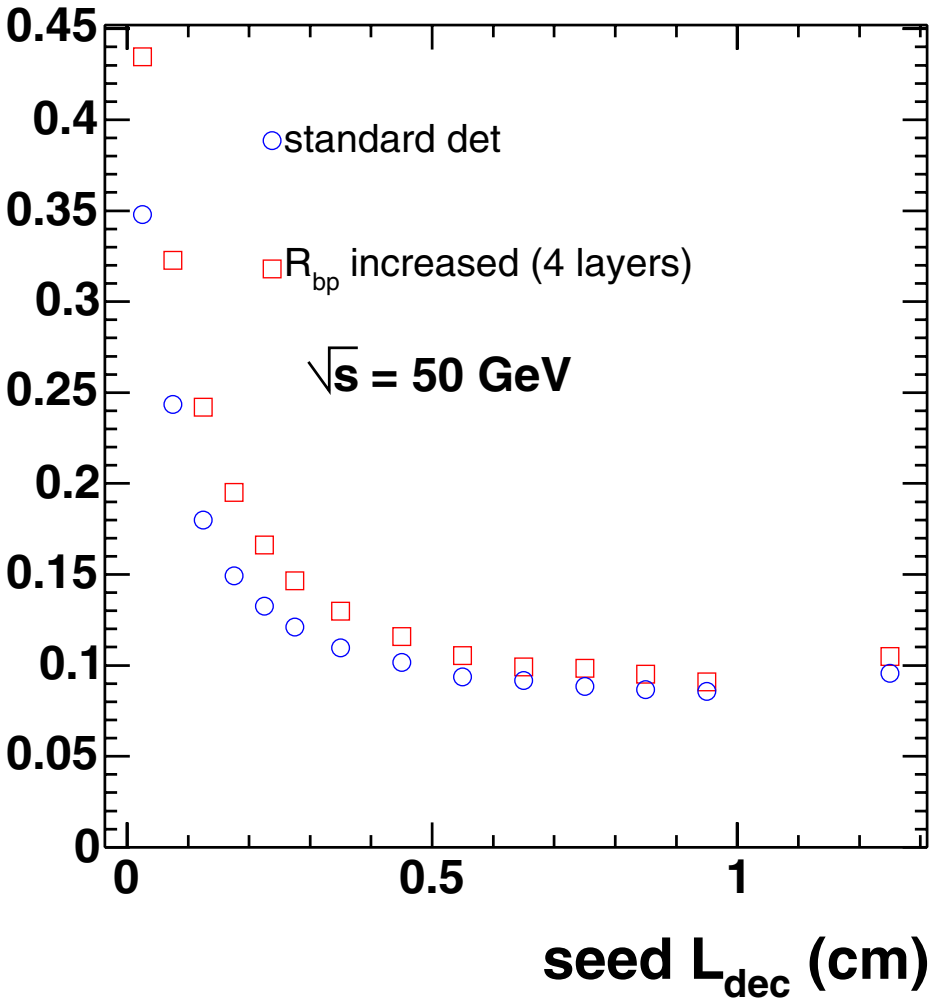

2- and 4-jet luminosity factors

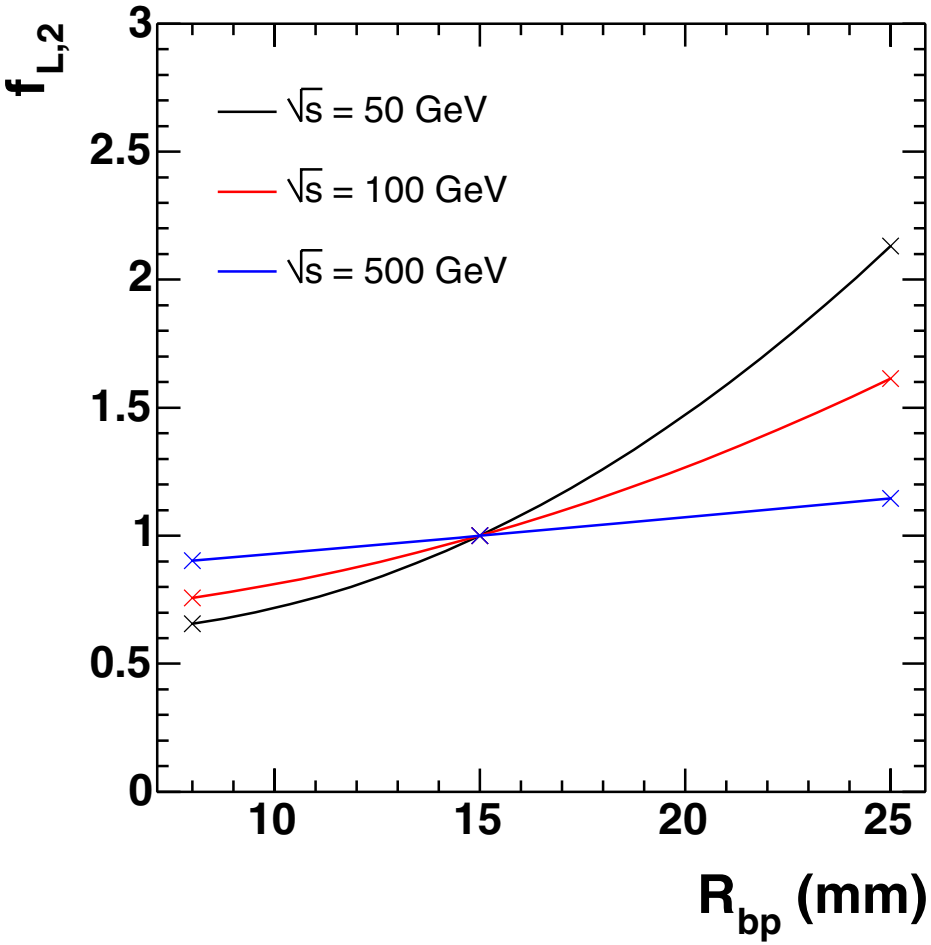

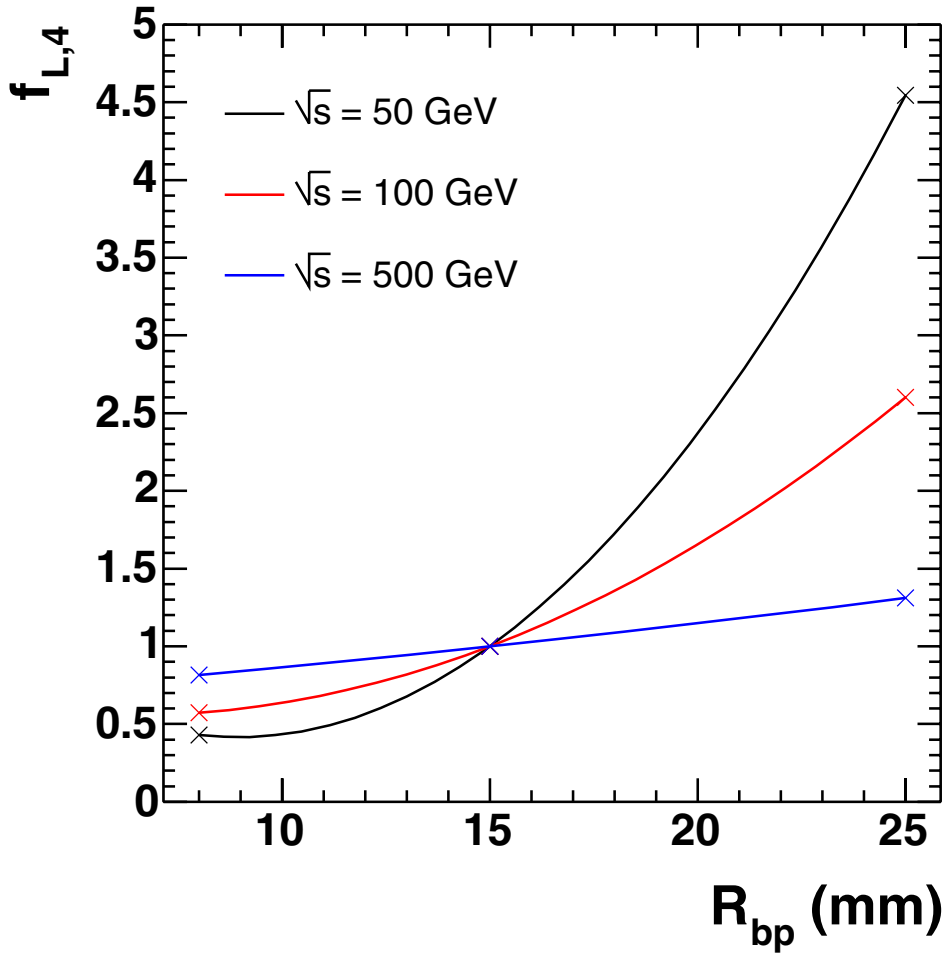

for channels depending on quark sign selection, significant increase in integrated luminosity required to compensate for increase in beam-pipe radius – NB further remarks next page!

Further remarks on translating to luminosity

- This simplified method for translating into luminosity shows the trends, but somewhat exaggerates the detector dependence.

- better procedure is to weight events according to their significance, as function of L_{dec}.

- Comparison with very preliminary (last Sunday) hand calculation for sqrt(s) = 50 GeV

  2-jet luminosity factor: by cut: 2.14

  by event weighting: 1.65 – 1.85 (background dependent, background >= 10 assumed)

- No change in the conclusions: significant advantage for physics of detector with smaller beam pipe

Comparison with SiD and GLD vertex detectors

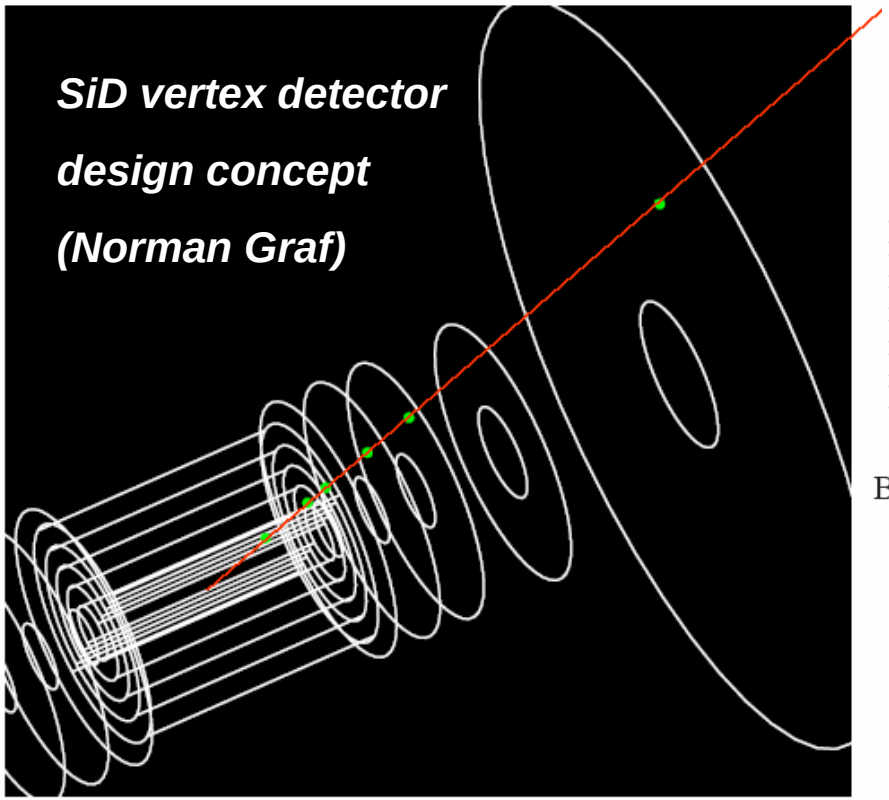

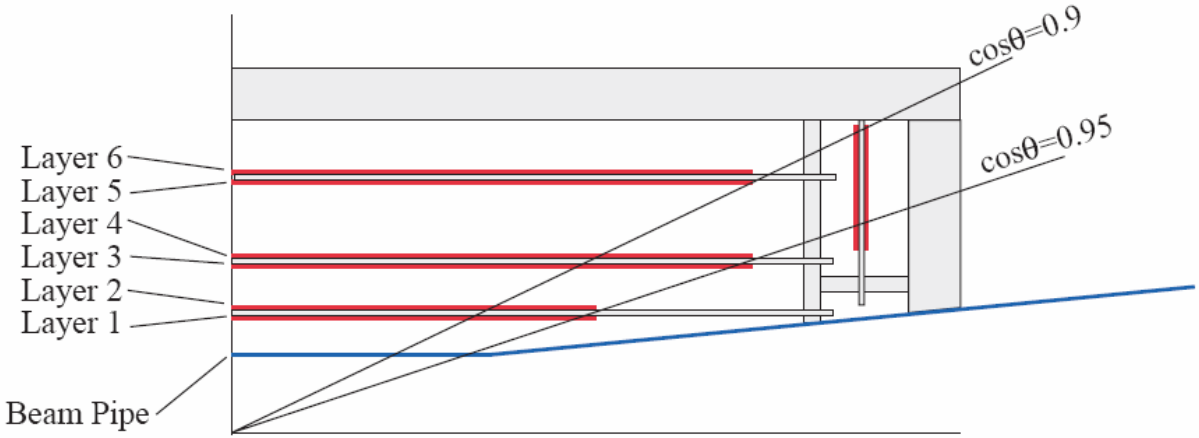

GLD vertex detector design (one quadrant)

- For comparison, both vertex detectors have been inserted into same 'global' detector geometry as LDC vertex detector, to decouple vertex detector performance from other effects

- BUT: effects such as degradation of point resolution at oblique angles and radial shifts of barrel staves not taken into account: could degrade performance more strongly for LDC than for SiD

Comparison with SiD & GLD vertex detectors: Results

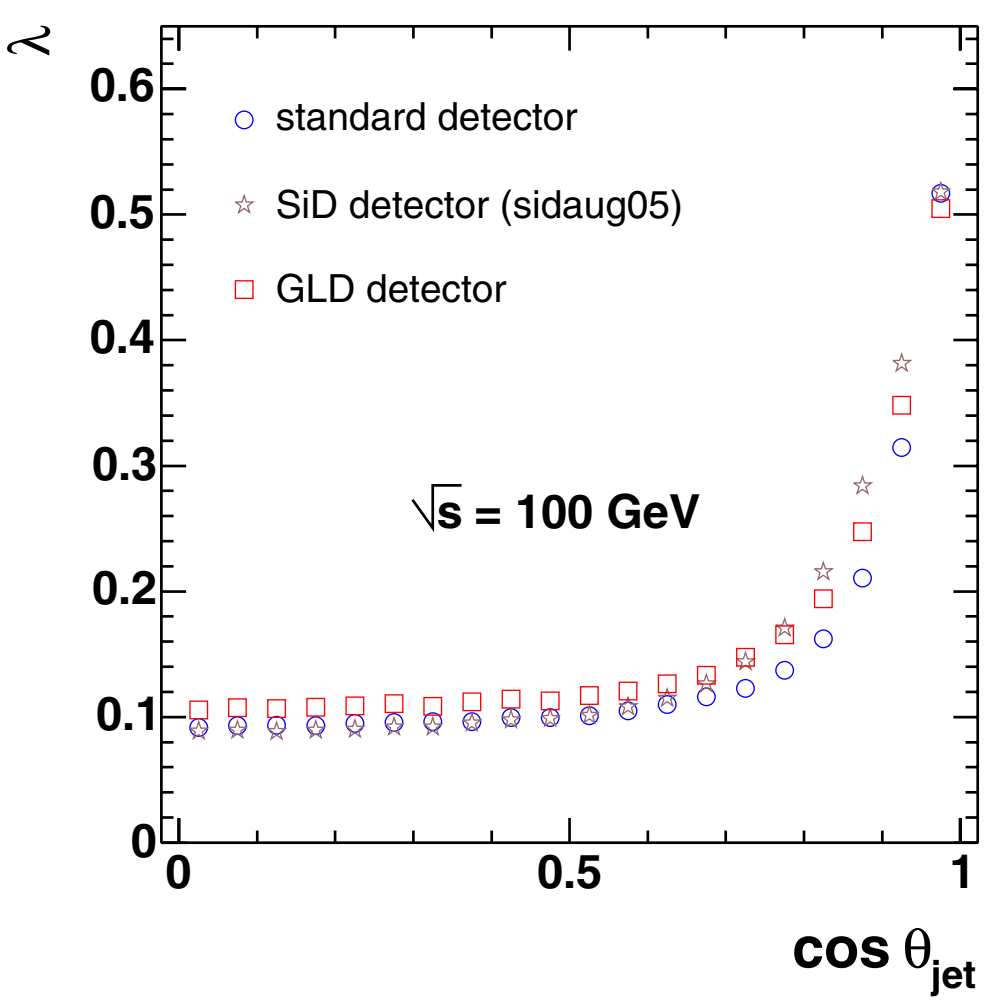

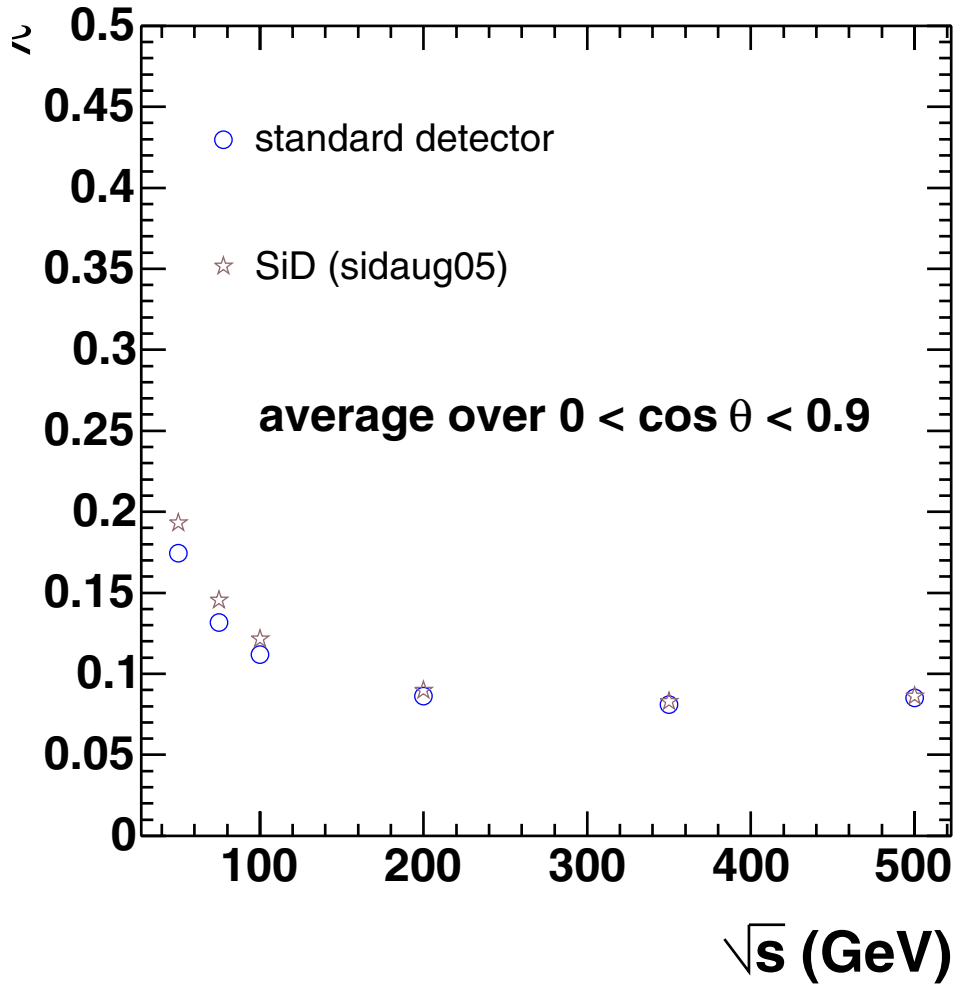

- material at the end of SiD short barrel staves compromises performance at large cos θ
- GLD performance affected by larger beam pipe radius compared to 'standard' detector

Summary

- b quark sign selection is a powerful physics tool, which will greatly enhance sensitivity to new physics – studied for the 40% of cases yielding charged B hadrons, by measuring their vertex charge
- performance is determined by probability of reconstructing a neutral B-hadron as charged
- this measurement is sensitive to multiple scattering in the vertex detector (low momentum tracks in the decay chain become merged with the IP)
- vertex detectors with beam pipe radii ranging from 8 – 25 mm have been compared; estimates indicate that for channels depending on quark sign selection, a significant increase in integrated luminosity would be required to compensate for an increase in beam-pipe radius
- The short-barrel plus endcaps vertex detector of the SiD concept degrades at lower cos θ than the LDC long-barrel vertex detector, due to the larger amount of material towards the central part of the detector;
  GLD vertex detector performance is affected by the larger radius of the innermost detector layer, dictated by pair-background extending further out in the lower B-field of the GLD detector

Conclusions

- It is important that the final focus design should respect the baseline beam pipe radius of 12-15 mm.

- R&D to reduce beam pipe thickness to 0.4 mm and vertex detector layer thickness to 0.1% X_0 is important.

- Higher solenoid field is important, since acceptable pair background rates on layer 1 need to be achieved.

Additional Material

Typical event processing at the ILC

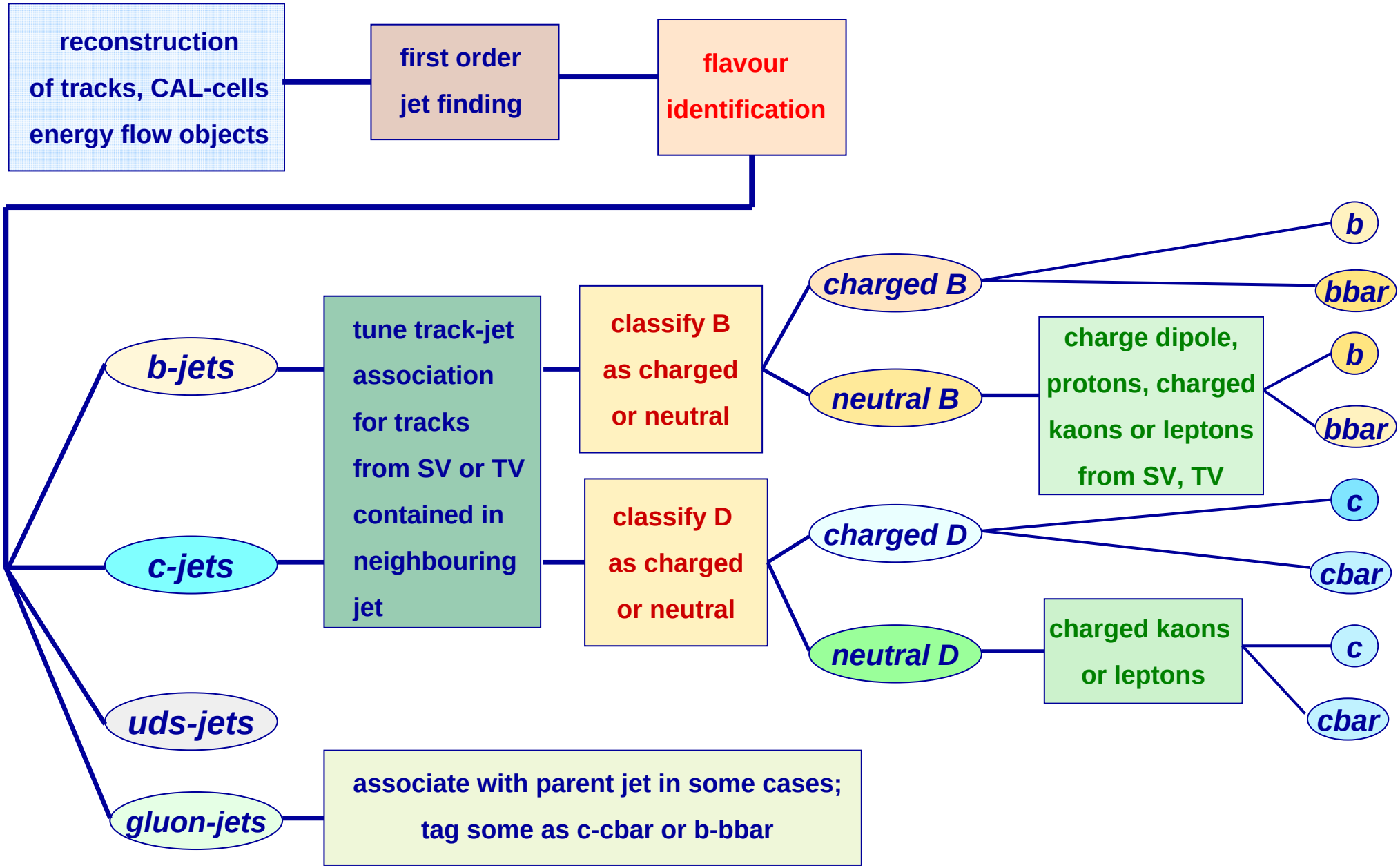

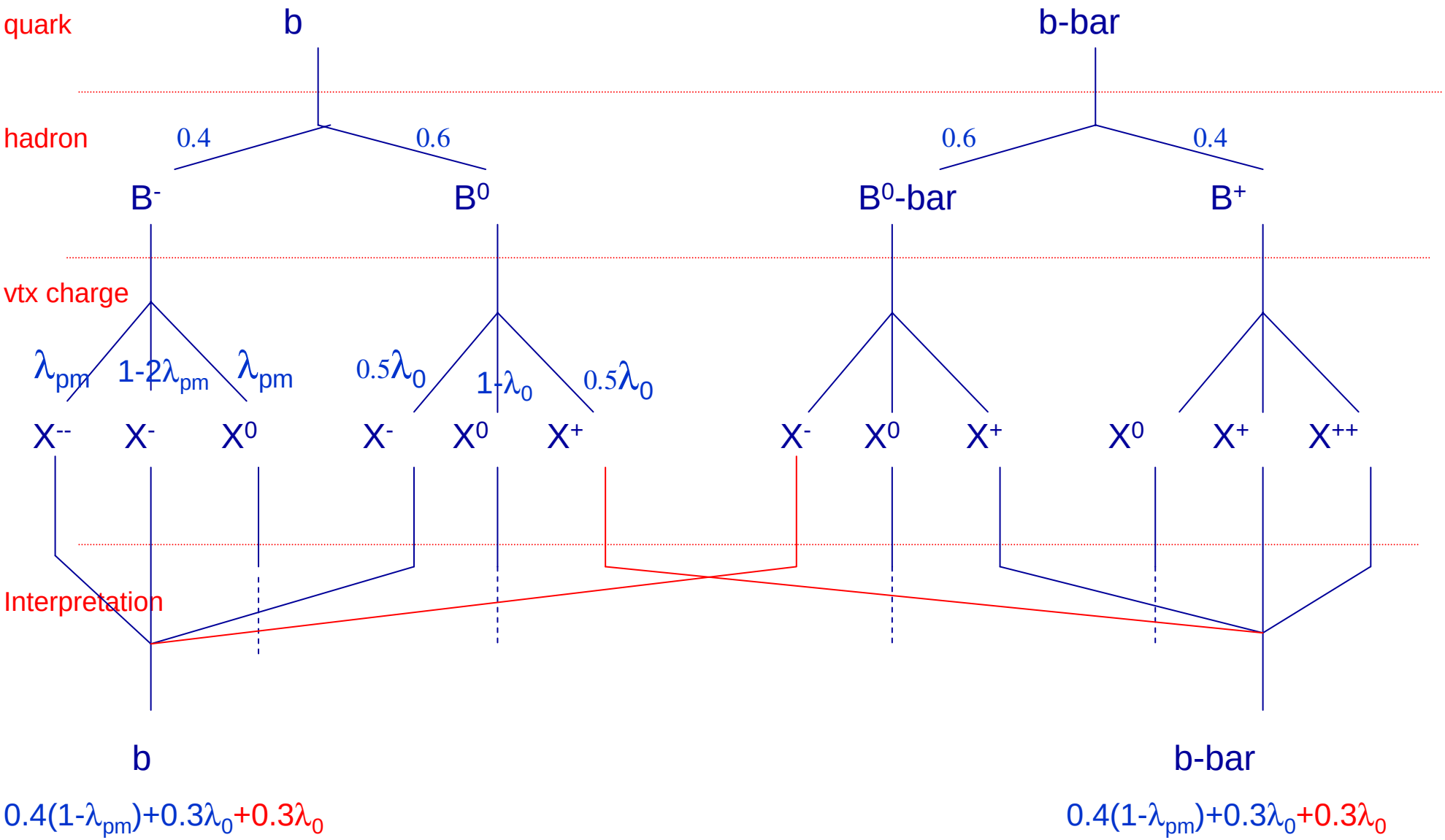
quark
b
b-bar
hadron
0.4
0.6
0.6
0.4
B-
B0
B0-bar
B+
vtx charge
λpm
1-2λpm
λpm
0.5λ0
1-λ0
0.5λ0
X--
X-
X0
X-
X0
X+
X-
X0
X+
X0
X+
X++
Interpretation
b
b-bar
0.4(1-λpm)+0.3λ0+0.3λ0
0.4(1-λpm)+0.3λ0+0.3λ0

Attempt at estimating effective luminosities from λ_0

with $\varepsilon_b(L_{dec} > 0.03$ cm, $R_{bp} = 15$ mm) the b-tag efficiency of the standard detector corresponding to the standard L_{dec} cut value and

$\varepsilon_b(L_{dec} > L_{dec,equiv}, R_{bp} = 25$ mm) that of the large R_{bp} detector at the point of equal λ_0

define 2-jet luminosity factor $f_{L,2}$ at $R_{bp} = 25$ mm as

$$f_{L,2} = (\varepsilon_b(L_{dec} > 0.03\text{cm}, R_{bp}=15\text{mm}) / \varepsilon_b(L_{dec} > L_{dec,equiv}, R_{bp}=25\text{mm}))^2$$

4-jet luminosity factor $f_{L,4} = f_{L,2}^2$

and equivalently for the standard and the small R_{bp} detector

Adding a further layer to the R_{bp} = 2.5 mm detector

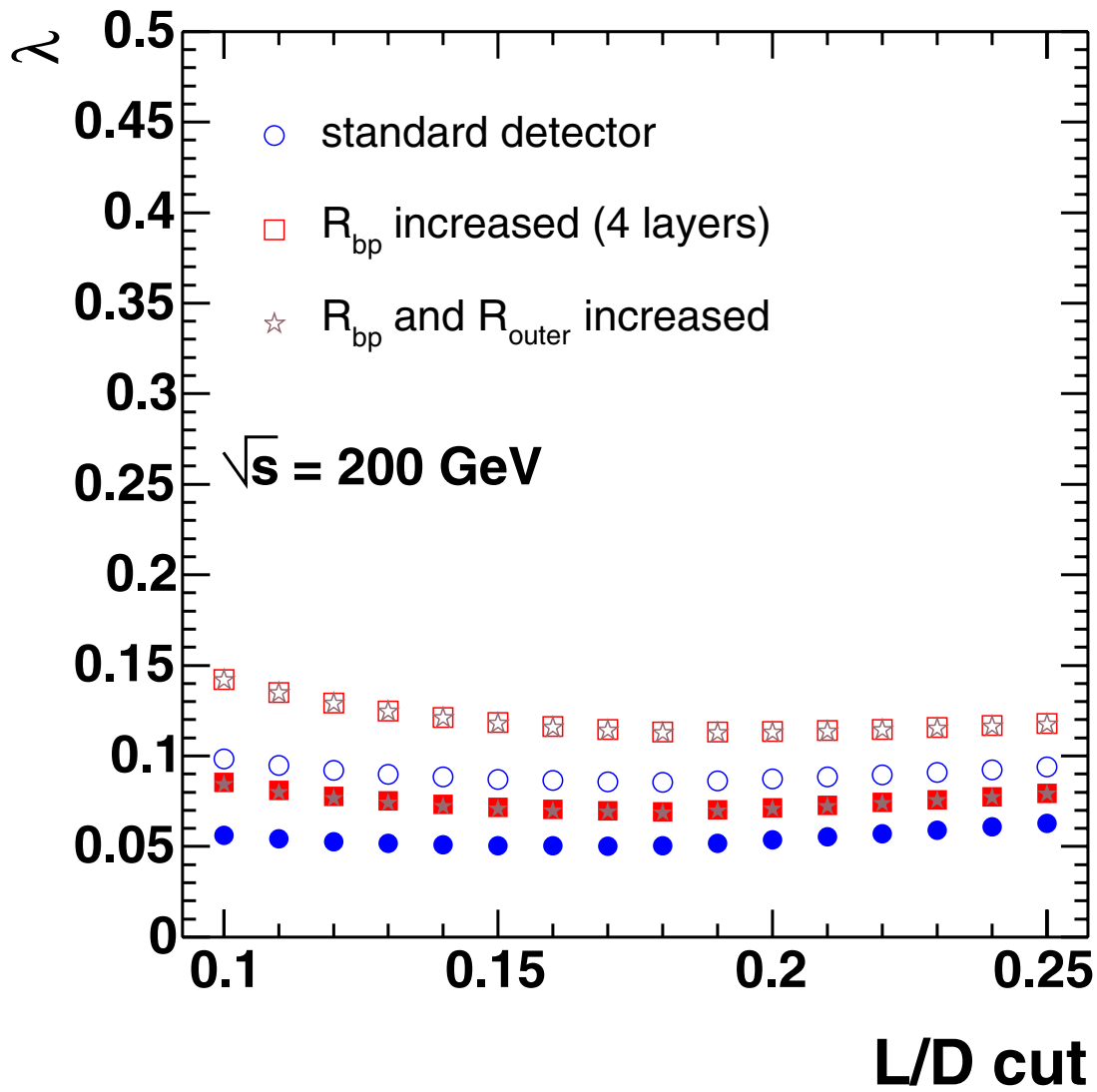

Increasing beam pipe thickness for standard detector

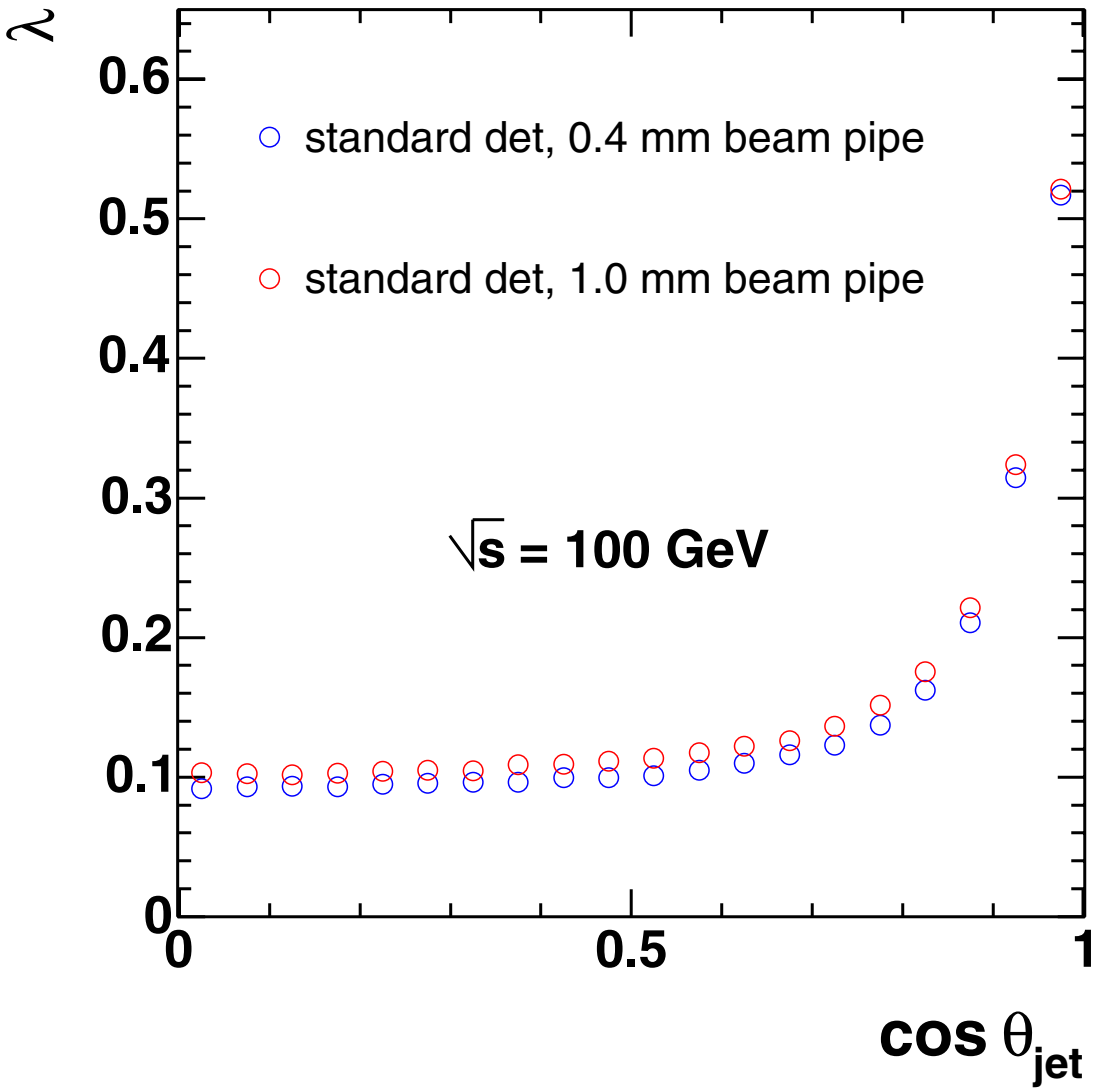

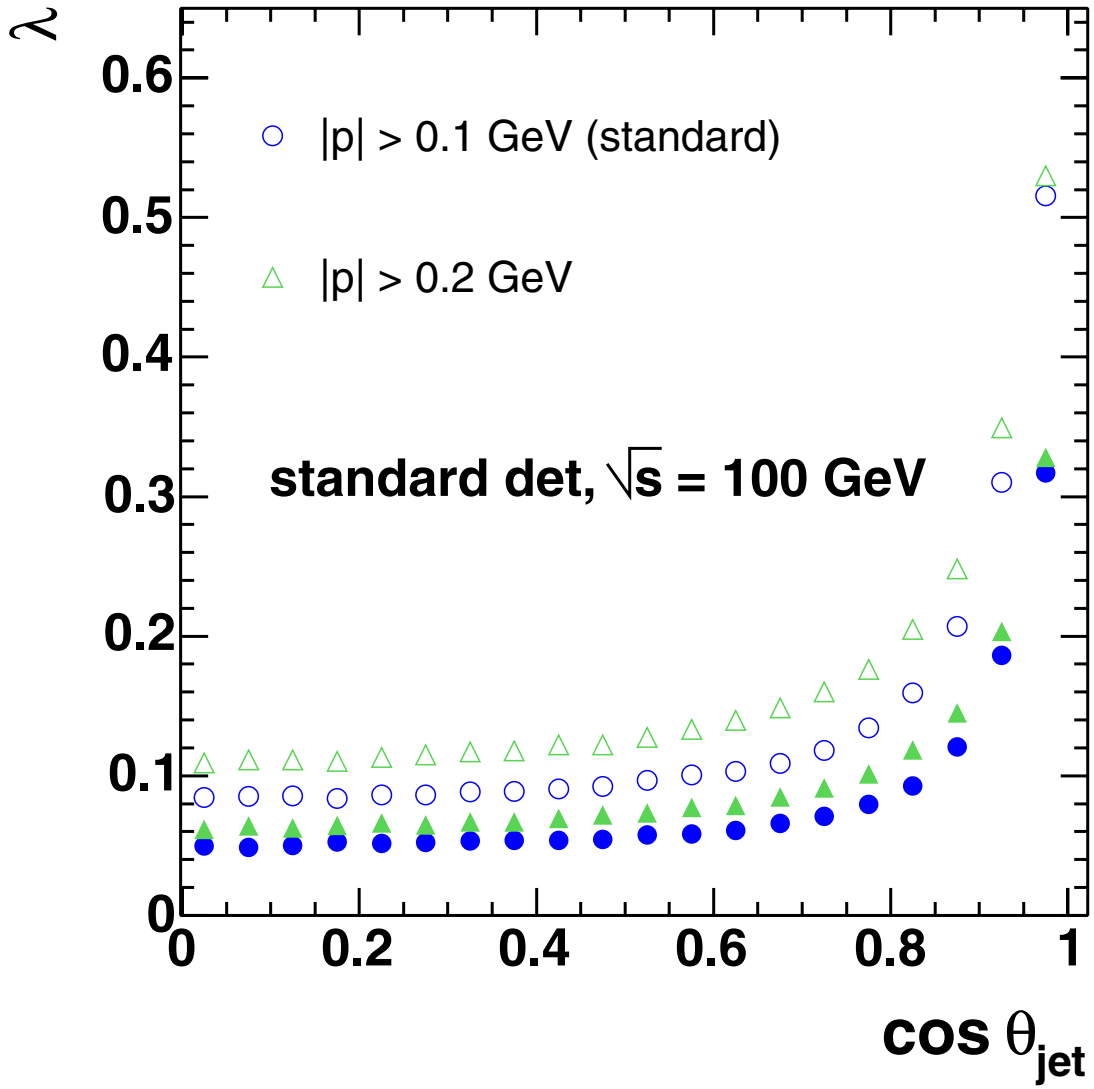
λ
0.6
0.5
0.4
0.3
0.2
0.1
0
|p| > 0.1 GeV (standard)
|p| > 0.2 GeV
standard det, √s = 100 GeV
0
0.2
0.4
0.6
0.8
1
cos θjet

L/D cut dependence in bins of seed decay length

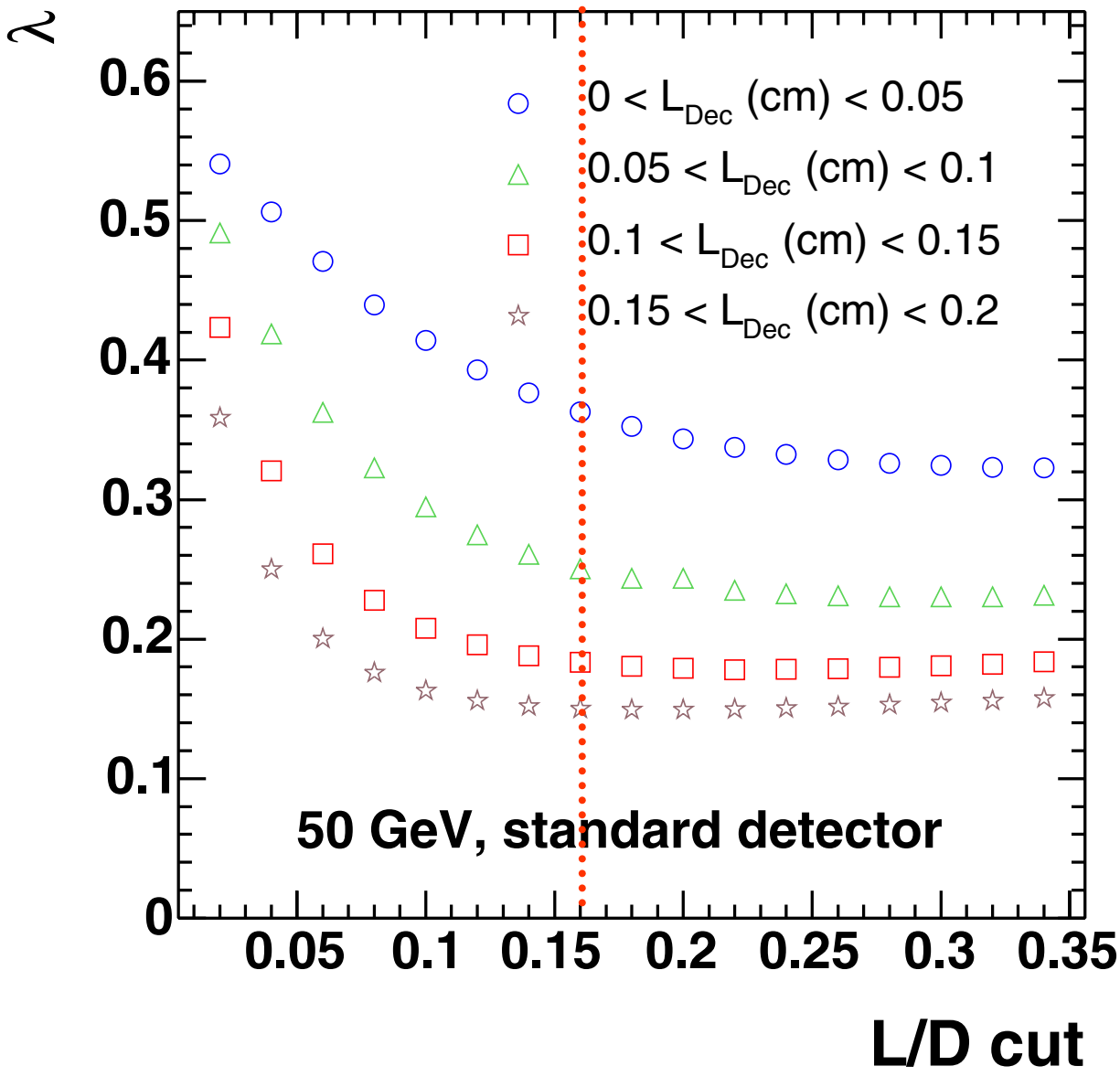

- decay length distribution peaks at much shorter distances from the IP for low than it does for high sqrt(s)

  → at low sqrt(s), performance more affected by backround from IP tracks and gluon splitting

- left: λ_0 as function of L/D cut, in four bins of seed decay length

- optimal L/D cut decreases as one moves away from the IP

  dotted line: standard cut value

Improvement obtained from variable L/D cut ?

dependence of λ_0 on L/D cut flat over wide range of L/D in each L_{dec} bin

→ only first two L_{dec} bins show difference in λ_0 when moving from const to variable L/D cut

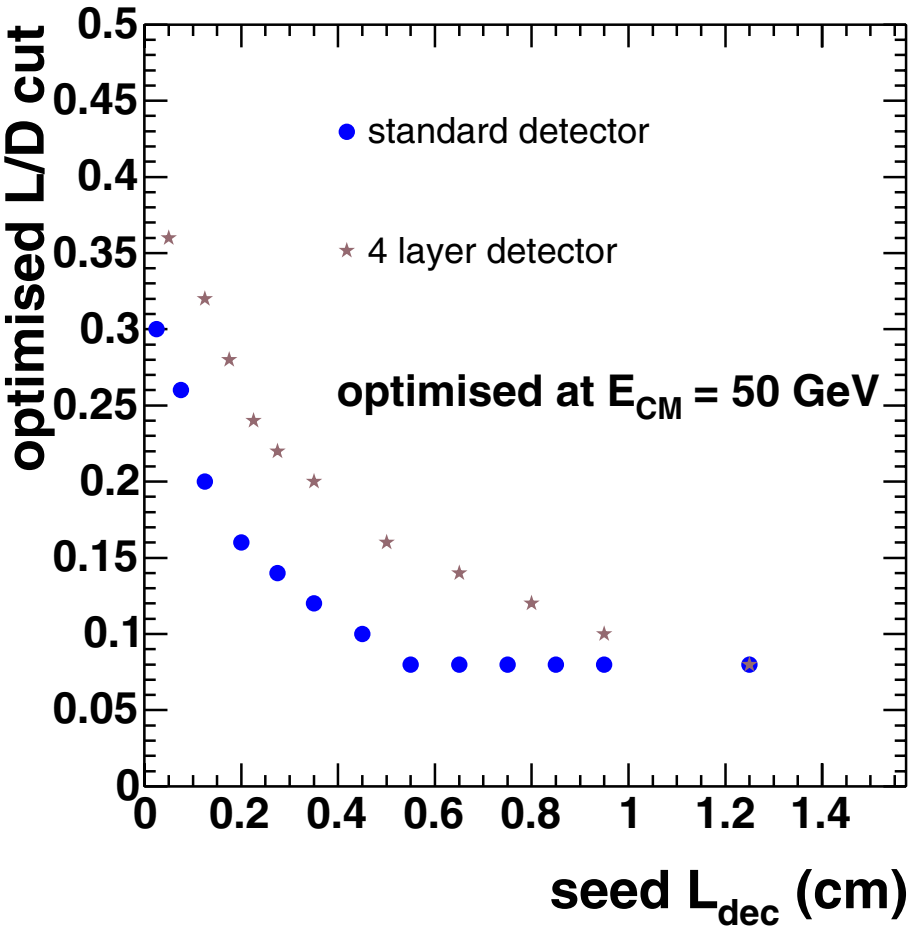

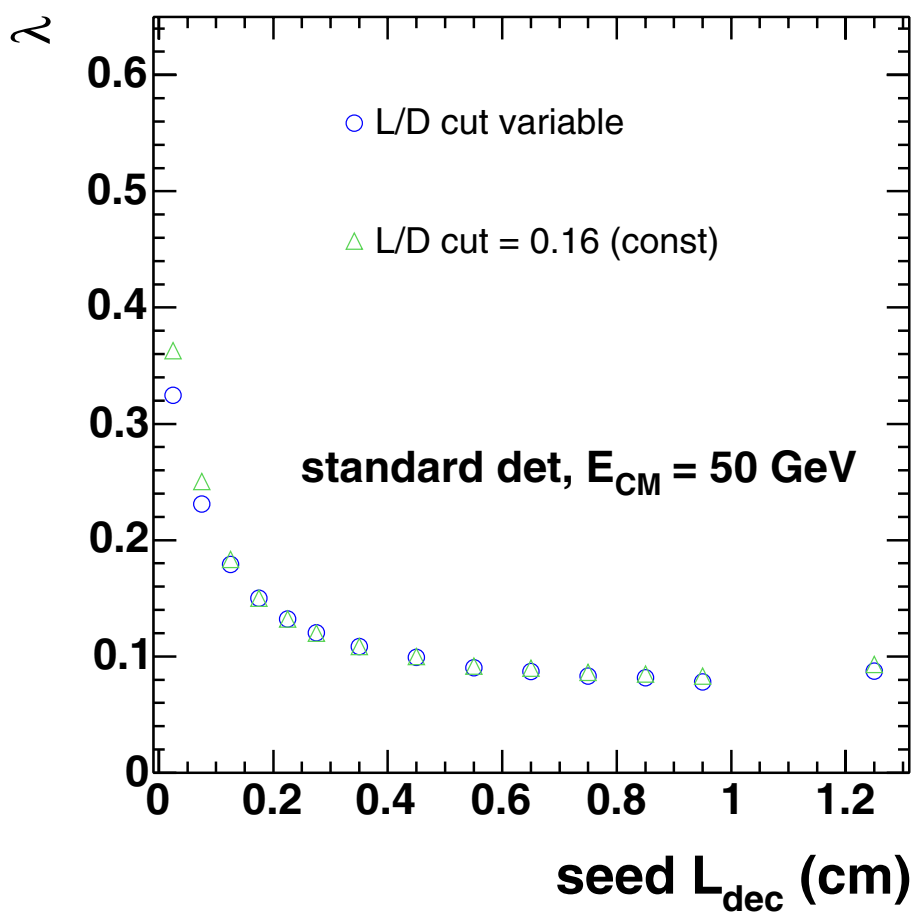

change in resulting λ_0, integrated over L_{dec}, at the permille level → NOT USED

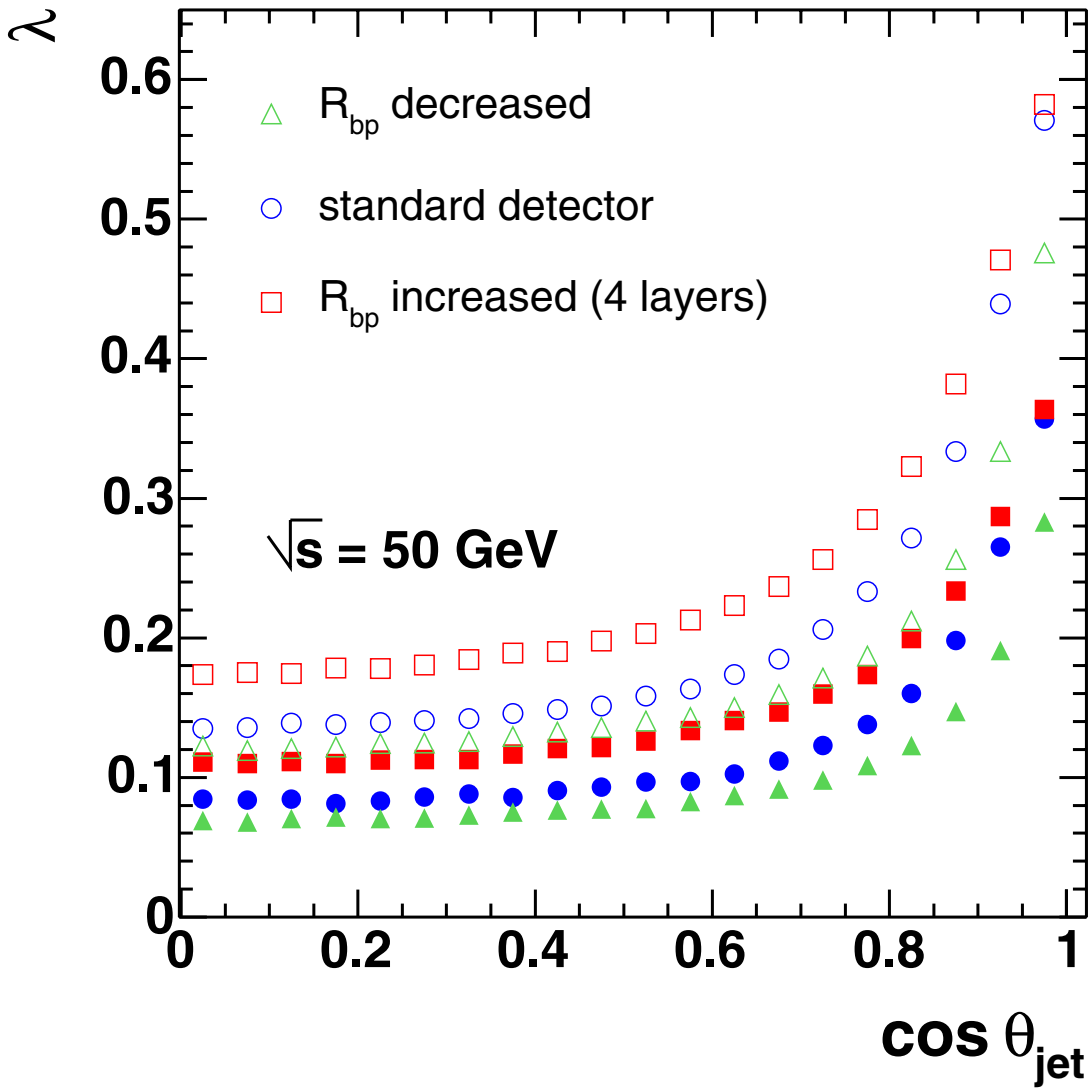
λ
0.6
0.5
0.4
0.3
0.2
0.1
0
0
0.2
0.4
0.6
0.8
1
R_bp decreased
standard detector
R_bp increased (4 layers)
√s = 50 GeV
cos θ_jet

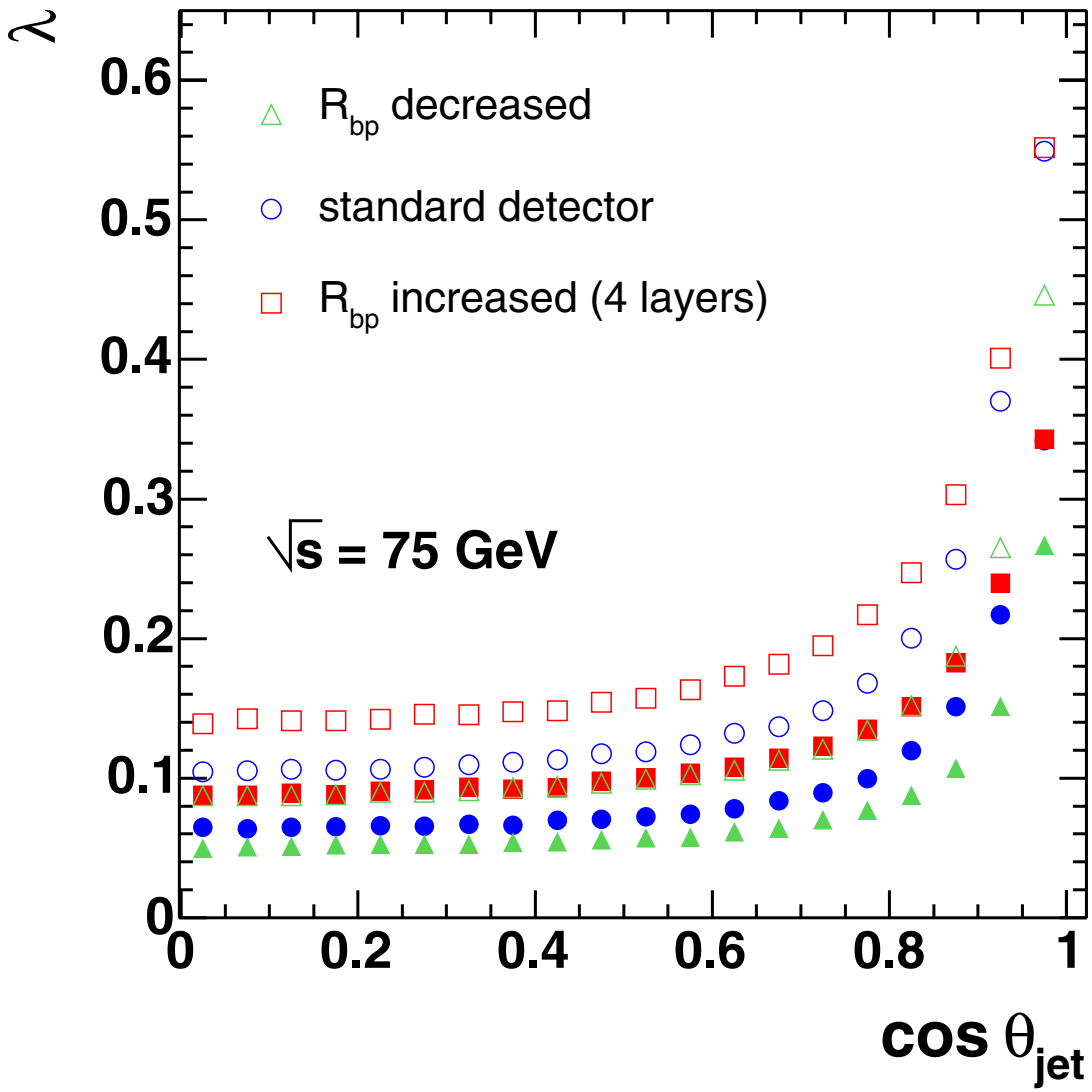
λ
0.6
0.5
0.4
0.3
0.2
0.1
0
0
0.2
0.4
0.6
0.8
1
R_bp decreased
standard detector
R_bp increased (4 layers)
√s = 75 GeV
cos θ_jet

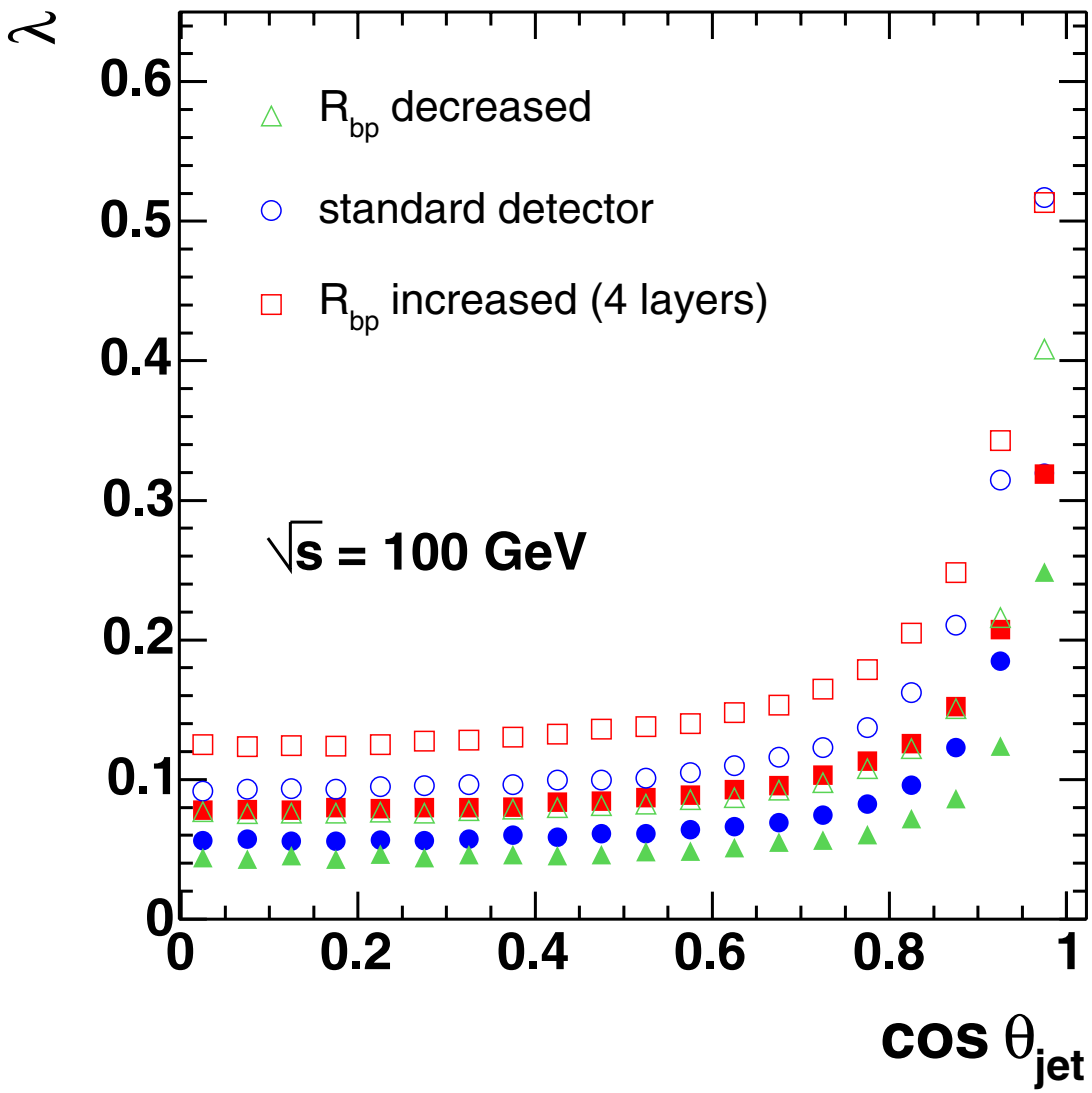
λ
0.6
0.5
0.4
0.3
0.2
0.1
0
0
0.2
0.4
0.6
0.8
1
R_bp decreased
standard detector
R_bp increased (4 layers)
√s = 100 GeV
cos θ_jet

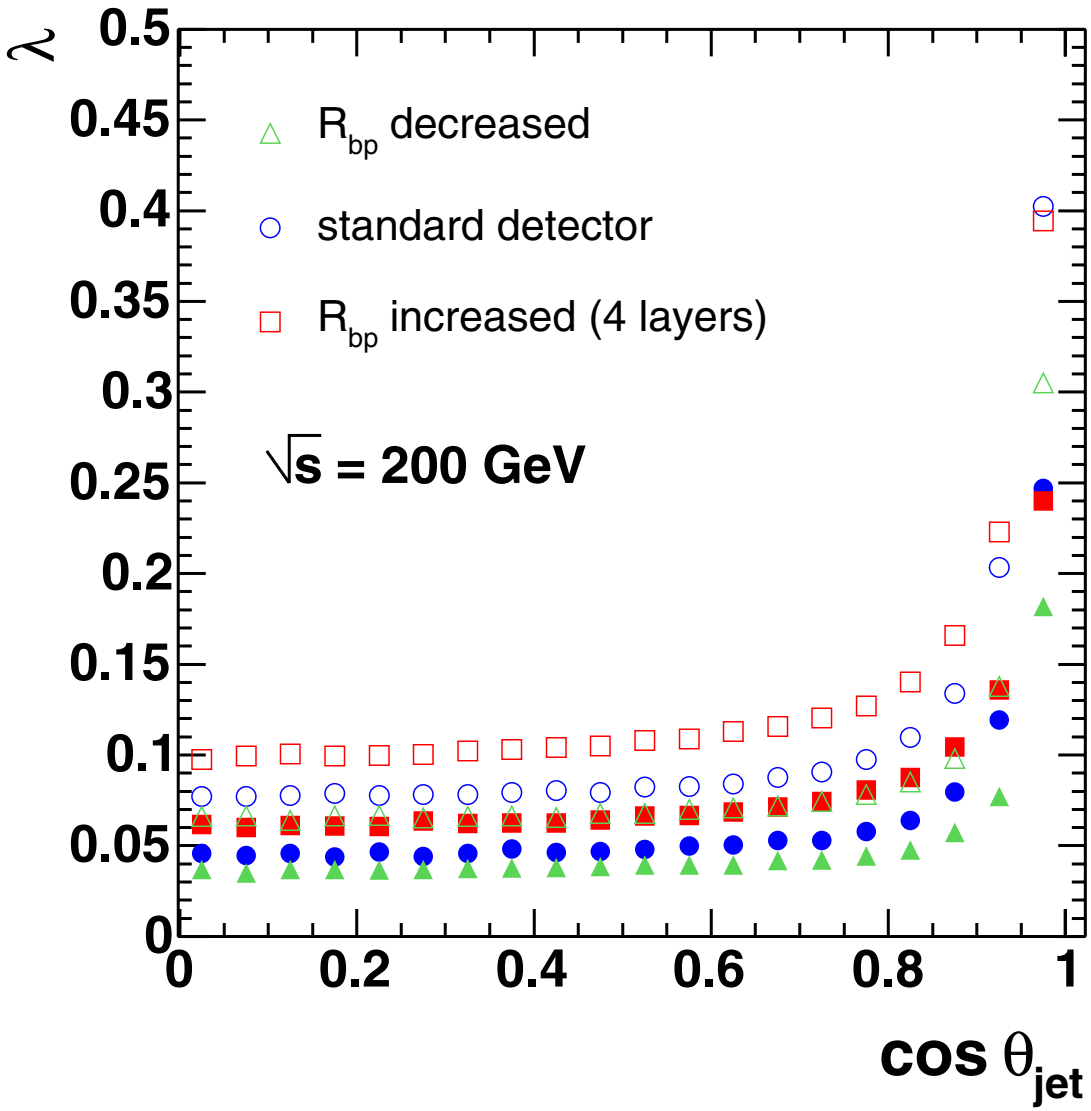
λ
0.5
0.45
0.4
0.35
0.3
0.25
0.2
0.15
0.1
0.05
0
0
0.2
0.4
0.6
0.8
1
cos θjet
Rbp decreased
standard detector
Rbp increased (4 layers)
√s = 200 GeV

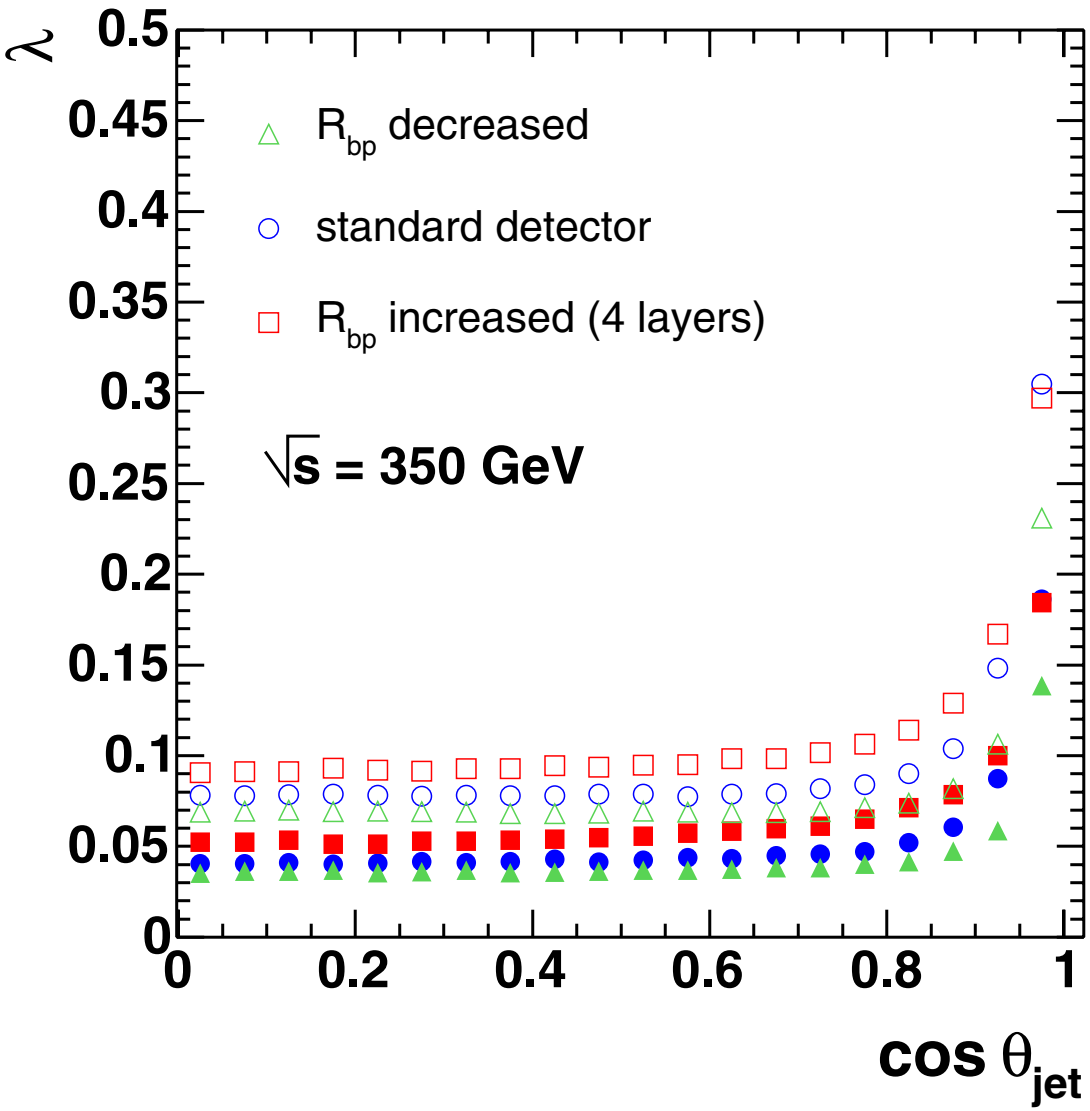
λ
0.5
0.45
0.4
0.35
0.3
0.25
0.2
0.15
0.1
0.05
0
0
0.2
0.4
0.6
0.8
1
R_bp decreased
standard detector
R_bp increased (4 layers)
√s = 350 GeV
cos θ_jet

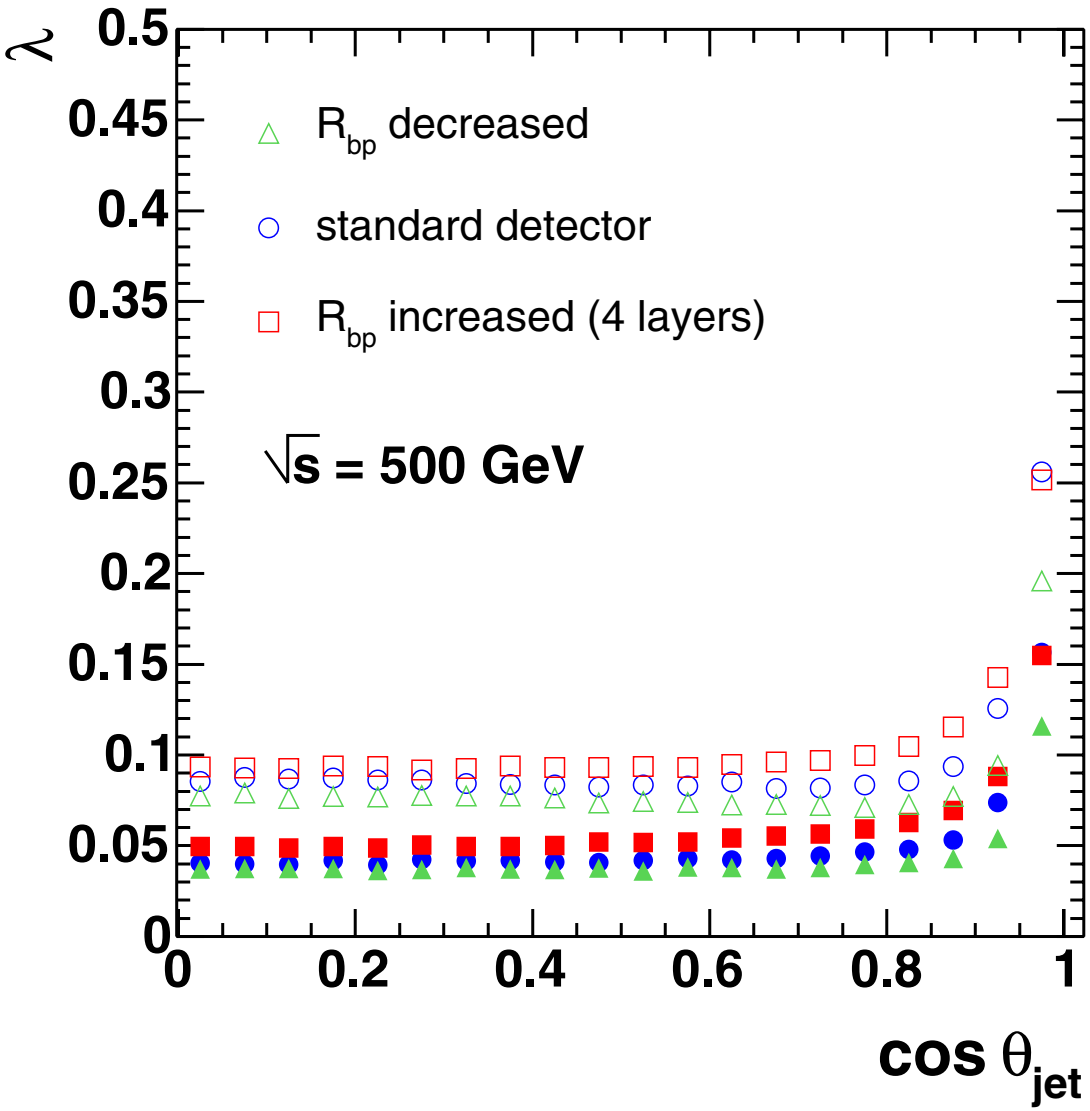
λ
0.5
0.45
0.4
0.35
0.3
0.25
0.2
0.15
0.1
0.05
0
R_bp decreased
standard detector
R_bp increased (4 layers)
√s = 500 GeV
0
0.2
0.4
0.6
0.8
1
cos θ_jet

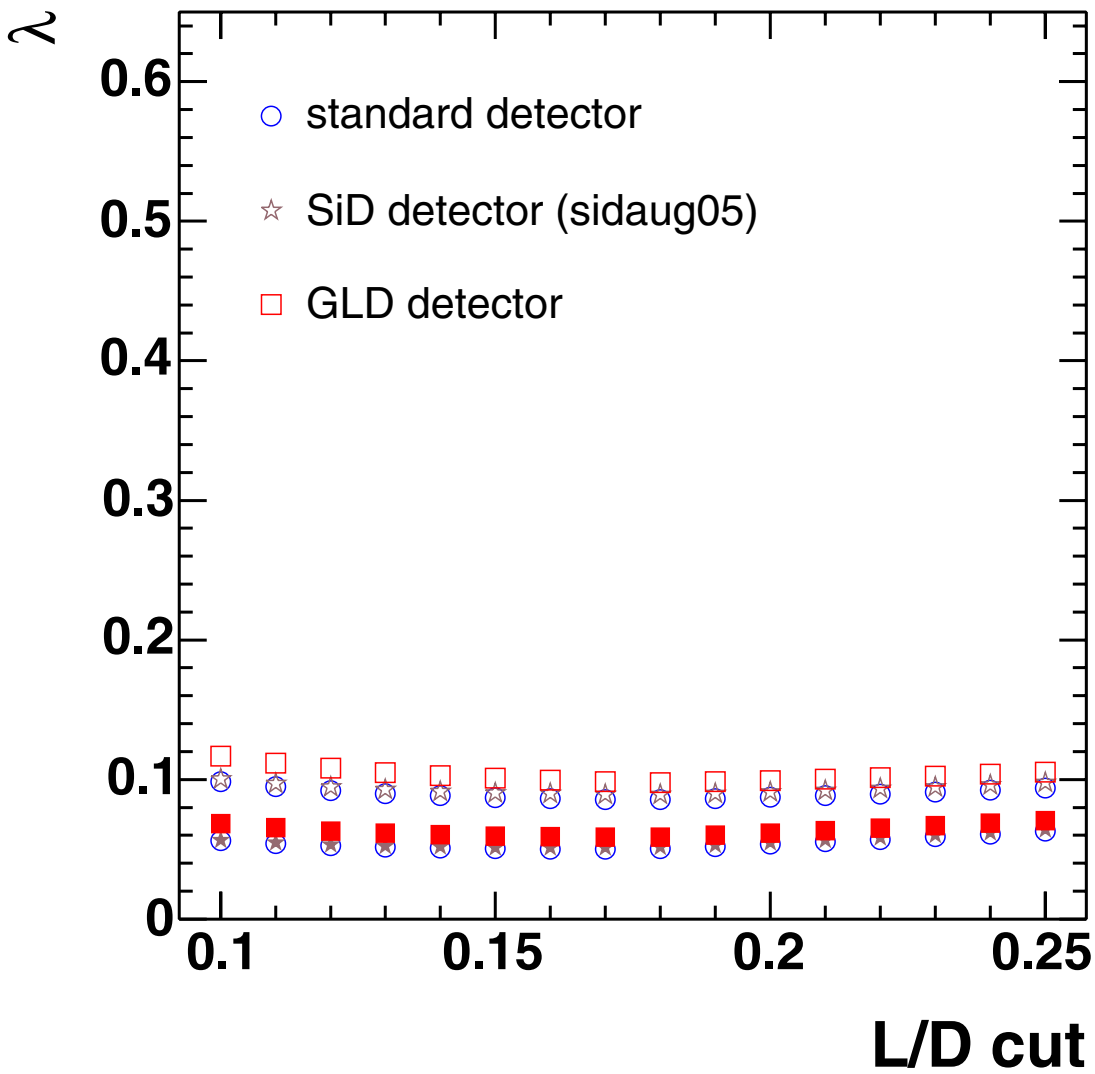
λ
0.6
0.5
0.4
0.3
0.2
0.1
0
standard detector
SiD detector (sidaug05)
GLD detector
0.1
0.15
0.2
0.25
L/D cut